GCAGS JOURNAL
A Publication of the Gulf Coast Association of Geological Societies
www.gcags.org

# Pore Networks and Reservoir-Quality Trends in Lower Cretaceous Carbonates of the Northern Rim of the Gulf of Mexico: Substantiating Reservoir-Quality Risk Factors

**Robert G. Loucks**

*Bureau of Economic Geology, Jackson School of Geosciences, University of Texas at Austin, University Station, Box X, Austin, Texas 78713–8924, U.S.A.*

## ABSTRACT

**Understanding the relationship between reservoir quality and associated parameters, such as depth, temperature, and pressure, is important for developing valid risk factors relative to reservoir quality in carbonate plays. To develop concepts that aid in understanding and calculating reservoir-quality risk factors for the onshore northern rim of the Gulf of Mexico, a large statistical database with over 21,000 core-plug porosity and permeability data points was constructed. Each data point is associated with parameters such as location, formation, depth, temperature, and pressure.**

**Graphs constructed from the database document how reservoir quality varies with depth and temperature for all the combined Gulf of Mexico data and for data separated by 6 geographic zones along the northern rim of the Gulf of Mexico. These graphs can be used as "reality checks" on predicted values of reservoir quality for a given play. If the estimated values are higher than what the database shows, a sound scientific reason must be provided to account for the difference.**

**Reviews of nine case histories where the geology, pore types, and reservoir quality are known suggest two main reservoir-quality pore-network suites: macropore-dominated and micropore-dominated. The macropore network occurs at shallower depths (generally less than 12,000 ft [3660 m]) and has high reservoir quality that is related to an interparticle- and moldic-dominated pore network, whereas the micropore network occurs at deeper depths (generally greater than 12,000 ft [3660 m]) and is related to a variety of micropores.**

**Large statistical databases, integrated with geologic parameters, provide insights into reservoir quality under varying burial environmental conditions. These insights support choosing a realistic risk factor for a particular play.**

## INTRODUCTION

Reservoir quality (porosity and permeability) is a key risk factor in exploring and producing hydrocarbons. Along the northern Gulf of Mexico rim (Fig. 1), the Lower Cretaceous is dominated by carbonates (Fig. 2), especially limestones. These carbonates have undergone alteration through a spectrum of diagenetic pathways into the subsurface that have produced a broad variety of pore networks and associated reservoir quality. Geothermal gradient varies from the Texas-Mexico border to southern Florida affecting thermal diagenesis of the carbonates, which in turn has affected reservoir quality.

Copyright © 2019. Gulf Coast Association of Geological Societies. All rights reserved.

Manuscript received February 12, 2019; revised manuscript received June 6, 2019; manuscript accepted June 15, 2019.

GCAGS Journal, v. 8 (2019), p. 35–56.
DOI: pending

To understand the pore networks and associated reservoir quality along the onshore northern rim of the Gulf of Mexico, two datasets are employed: (1) cores for the delineation of pore networks and (2) core-plug porosity and permeability analyses to establish magnitude of vertical and lateral trends of reservoir quality. This study utilizes petrographic data from numerous carbonate cores where pore networks have been described. In addition, a large digital database, consisting of core-plug analyses from 219 wells (Fig. 2), was constructed. The database is composed of 21,127 core-plug-porosity analyses and 20,250 core-plug-permeability analyses, which document the pore networks that influence the large range of porosities and permeabilities seen in the Lower Cretaceous Gulf of Mexico carbonates as well as vertical and regional trends in reservoir quality. As can be seen in Figure 1, the area of investigation in divided into 6 geographic zones.

Specific objectives of this investigation are to (1) document the variety of pore types and pore networks seen in the major Gulf of Mexico carbonate units; (2) provide statistical graphic summaries of porosity and permeability subdivided by depth,

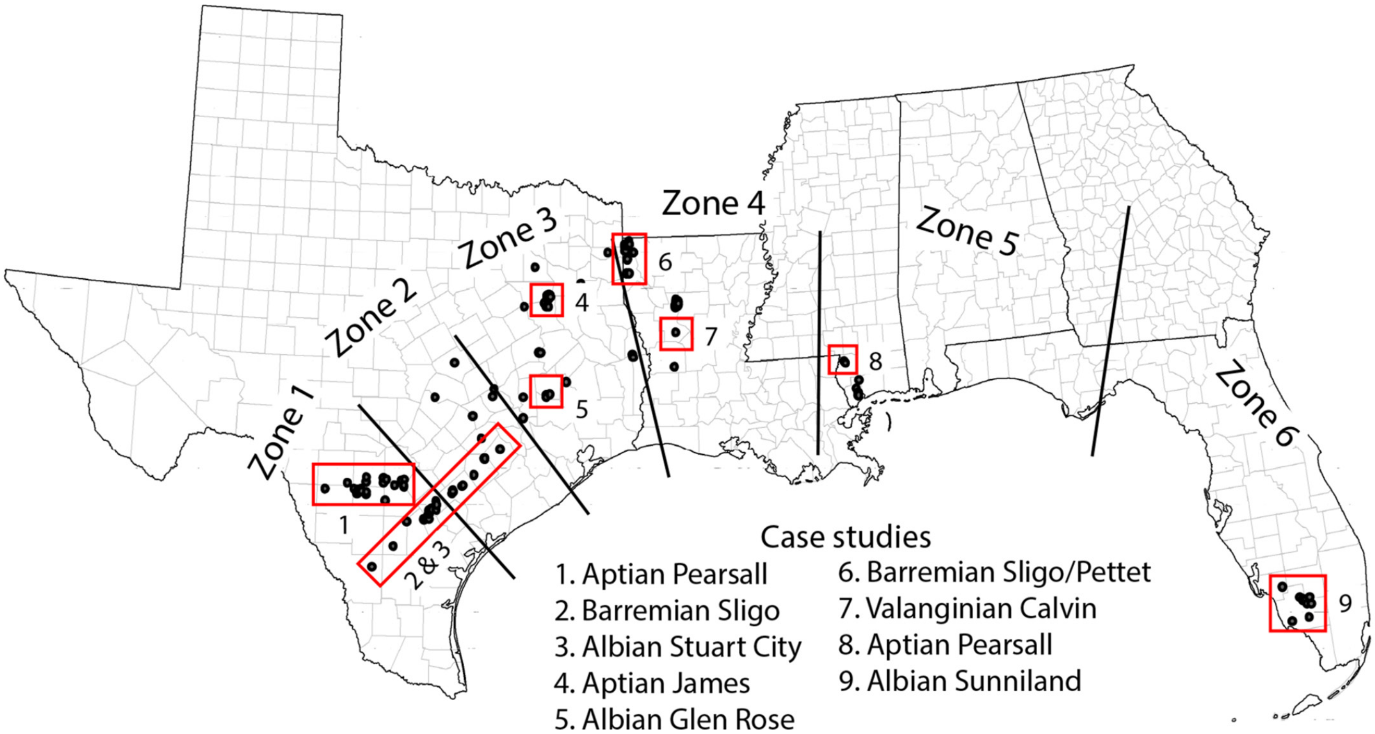


**Figure 1. Map of the northern rim of the Gulf of Mexico. The map is divided into 6 geographic areas in order to compare regional reservoir-quality trends. Wells with core-plug data are shown. Case study areas are outlined and labeled.**

temperature, and regional trends; (3) review case examples for selected formations where pore types and reservoir quality are integrated; and (4) discuss the use of these data for substantiating risk decisions for exploration and production management. These data provide real-world analyses associated with known parameters and will help predict reservoir quality where limited data are available.

## DATA AND METHODS

This investigation is based on rock data as observed and analyzed in cores. These data extend from the Texas-Mexico border in the west to the southern Florida area in the east (Fig. 1). Two types of rock data are employed here: (1) microphotograph and image data from thin-section petrography and scanning electron microscopy (SEM) imaging, and (2) core-plug porosity and permeability analyses.

Thin-section petrography defines the pore networks present within the carbonates. In this study, no new cores were analyzed; numerous studies of Gulf of Mexico carbonates are available in the literature, many completed by the present author or other coauthors. The data collected from the literature when integrated with data from the present investigation (thin sections core-plug measurements) are useful for documentation of pore networks and associated reservoir quality for several representative Gulf of Mexico formations. All thin sections were impregnated with blue-dyed epoxy to emphasize macropores (greater than 10 microns in diameter), and some were impregnated with blue-fluorescent dye to recognize micropores (l0 microns or less in diameter). Terminology of pore types generally follows that of Choquette and Pray (1970). Characteristics of macropores can be observed in thin sections using a petrographic microscope, but micropore size and shape must be characterized using the SEM. The blue-fluorescent dye impregnated thin sections can recognize micropores only by the blue haze observed under ultraviolet (UV) light.

The reservoir quality of the northern onshore Gulf of Mexico is documented by over 21,000 core-plug analyses collected over a 35 yr period, which has been compiled into a digital database by the Carbonate Reservoir Characterization Research Laboratory (RCRL) at the Bureau of Economic Geology, University of Texas at Austin. For each sample, the well name, American Petroleum Institute (API) number, location, depth, and geologic unit were recorded, and temperature and pressure were calculated based on data from associated wireline log headers.

Original core reports are not available to access confining pressures of measurement or if the samples were argillaceous or fractured. Some abnormally high-permeability samples with associated low porosities were eliminated or highlighted as probable fractured plugs. Also, no texture data were available to define the sample according to Dunham (1962) carbonate-texture classification. Samples depths came from data marked on cores or core boxes.

Corrected bottom-hole temperatures (BHT) were calculated for each core-plug analysis using wireline-log data according to Corrigan (2003). A ZetaWare web-based software program was available to do the BHT correction by inserting recorded BHT and time since circulation (ZetaWare, 2003). A geothermal gradient was then calculated based on corrected BHT and depth of log run. The geothermal gradient and mean-surface temperature was used to calculate a temperature for each core-plug sample. Wireline log headers were not available for approximately 5% of the wells, so geothermal gradients from nearby wells that penetrated the same formation were used.

Pressure at each core-plug sample depth was calculated from wireline log header mud weights using the following relationship: pressure (psi) = 0.052 × depth (ft) × drilling-fluid density (psi/ft) (Drilling Formulas and Drilling Calculations, 2018).

It is important to note that some of the formations have complex burial histories, during which the samples were buried deeper than where they were recovered. In South Texas, notably

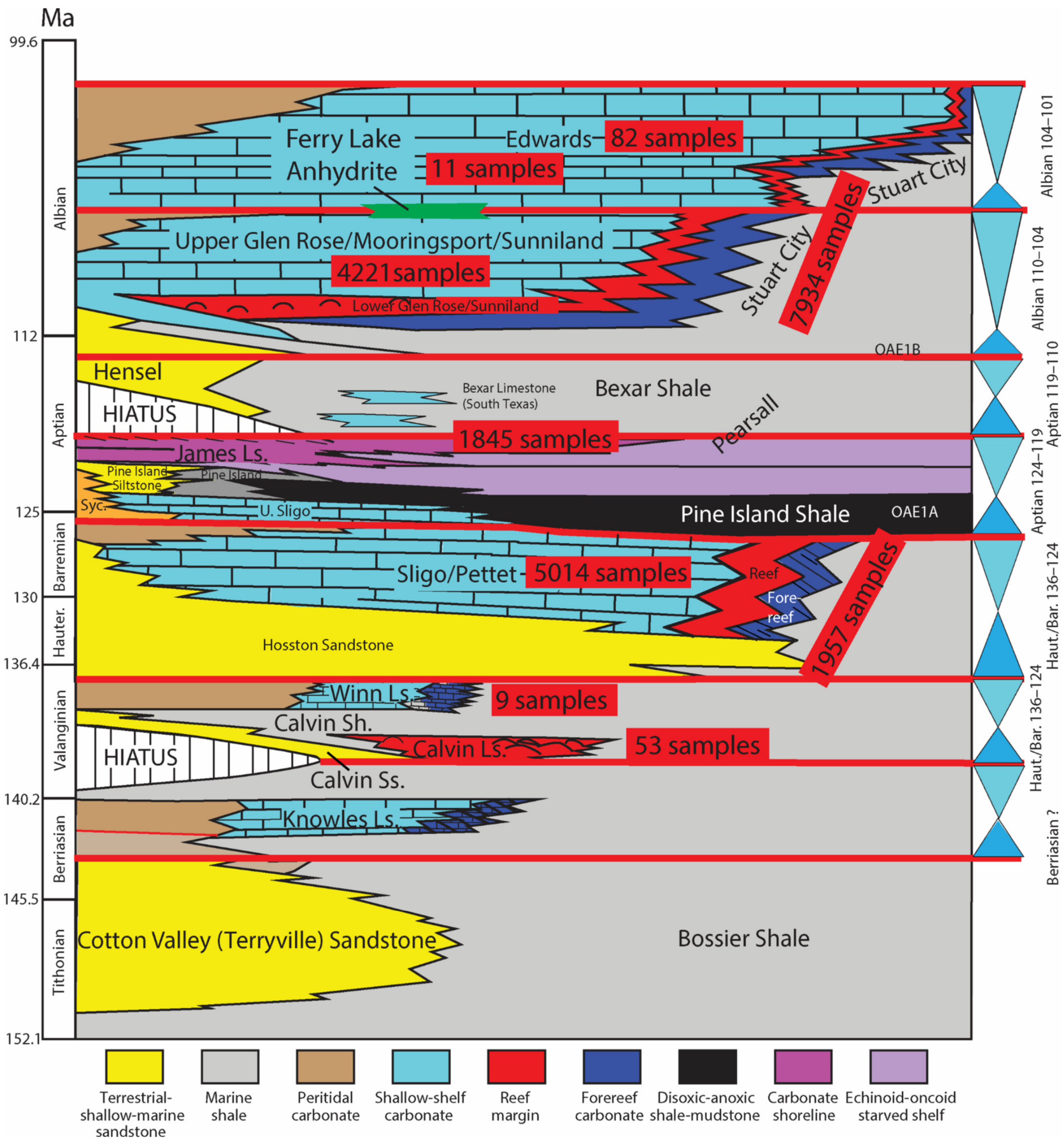


**Figure 2. Lower Cretaceous stratigraphic section along the northern rim of the Gulf of Mexico. The red boxes with number of samples refer to the number of core-plug porosity and permeability analyses from the associated formation. Stratigraphic section is modified after Loucks et al. (2017).**

southwestern Texas, some formations have had substantial uplift of as much as 6000 to 7000 ft (1829 to 2134 m) (Ewing, 2003); the area of the Sabine Uplift in East Texas also has a history of uplift (Ewing, 2009). The significance of uplift is that the strata have experienced higher temperatures and pressures while more deeply buried, which is important in understanding the thermal diagenetic state of the samples.

## GENERAL REGIONAL GEOLOGY

The Lower Cretaceous carbonates analyzed in this investigation were deposited on a broad carbonate-dominated platform where periodic influxes of siliciclastic sediments occurred. For detailed reviews of Lower Cretaceous deposition along the onshore northern rim of the Gulf of Mexico, see McFarlan and

Memes (1991), Phelps et al. (2013), and Loucks et al. (2017). The core-plug samples in this investigation range in age from Valanginian to Albian. Throughout this time period, at least four major shelf margins (Valanginian Calvin, Valanginian Winn, Barremian Sligo, and Albian Stuart City) (Fig. 2) having associated broad platforms with mixtures of carbonates and siliciclastic strata developed (McFarlan and Memes, 1991; Phelps et al., 2013; Loucks et al., 2017). The Aptian Pearsall carbonates and siliciclastics signify a time of a worldwide transgression (Loucks, 1977; Phelps et al., 2013). During the Lower Cretaceous, at least 6 composite sequences occurred on the northern Gulf of Mexico shelf, with durations ranging from 4 to 16 million yr (Phelps et al., 2013). These variations in sea level, along with multiple tectonic events, created a complex mosaic of both laterally and vertically heterogeneous lithofacies. These lithofacies span the spectrum of carbonate types and exhibit multiple types and degrees of diagenesis.

The geothermal gradient around the northern Gulf of Mexico varies, being higher in the west and lower in the east (Loucks et al., 1984; Forrest et al., 2005; Dutton et al., 2012). The variance has a regional effect on the intensity of diagenesis: higher geothermal gradients tend to advance diagenesis and commonly lower reservoir quality, whereas lower geothermal gradients have less effect on diagenesis and reservoir quality (Loucks et al., 1984; Dutton et al., 2012).

## PORE-NETWORK REVIEW

### Introduction to Carbonate Pore Networks

Porosity and permeability are directly related to pore type, pore abundance, and pore connectivity; permeability is also strongly controlled by pore-throat radius. Therefore, a review of pore networks observed in the Lower Cretaceous Gulf of Mexico carbonates is important for discussing reservoir quality. The approach used is based on original mineralogy of the carbonate sediment to simplify and organize the discussion. At the time of deposition, carbonate sediments consist of a combination of grains composed of calcite, aragonite, and Mg–calcite (e.g., Land 1967, 1970) (Fig. 3). One or two mineralogical types may dominate, each having different chemical stabilities and undergoing diagenesis differently under the same conditions (e.g., Land, 1967). Where matrix is absent, resulting pores within and between grains can have very different styles and sizes, and associated pore-throat sizes can vary greatly (e.g., Loucks, 2002). In general, primary pores are commonly only well preserved in grain-rich packstones, grainstones, and boundstones; these limestone textures are emphasized in this investigation. Dolomitization also affects pore development, but within this database, the majority of samples are limestone; only 2.2% of the samples are noted as dolomitic. In the following sections, each original mineralogy will be discussed relative to diagenesis of individual grains and also as carbonate bodies composed of these grains.

### Calcite Grain-Dominated Mineralogy

Many carbonate grains in the Lower Cretaceous—such as some mollusks (e.g., oysters and chondrodonts), serpulid worm tubes, some benthic and planktic foraminifers, and coccoliths—were originally calcite or very low Mg–calcite. Calcite grains are relatively stable in marine and meteoric waters and undergo little if any macrodiagenesis relative to dissolution that could create pores or add to cement in open pores between grains or within grain voids (e.g., Land, 1967). Because of the chemically stable character of calcite grains, carbonate sands and gravels dominated by calcite can be lacking in early cements, which promotes mechanical compaction (more-tightly packed grains and some mechanical breakage of grains) and chemical compaction (expressed as pressure solution at grain contacts) with burial (Fig. 4A). These units can lose a large amount of primary interparticle

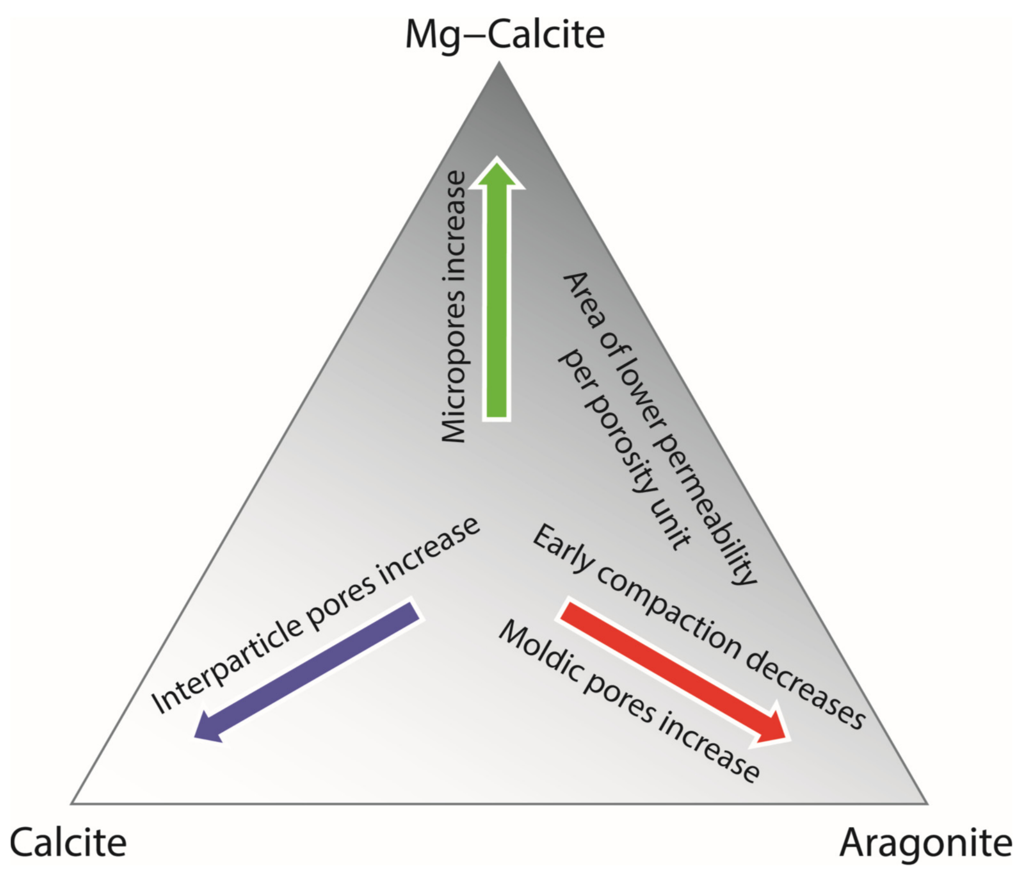


**Figure 3. Ternary diagram depicting the three major minerals that compose initial carbonate sediments and the expected impact on pore-network assemblages. Area of lower permeability per porosity units is related to micropore development associate with Mg–calcite diagenesis and cementation associated with aragonite diagenesis.**

pores during burial; additionally, if no aragonite grains were present, moldic pores were unlikely to form. However, if pore fluids are saturated in calcium carbonate during early or shallow-burial diagenesis, cement can form around the grains, creating a rigid framework that aids in preserving interparticle pores (Fig. 4B) that may still be well connected and form an effective primary pore network.

### Aragonite Grain-Dominated Mineralogy

Aragonite grains in the Early Cretaceous marine environment—including bivalves, gastropods, green algae, corals, and cephalopods—were extremely common, as were aragonite ooids (e.g., Flügel, 2004; Scholle and Ulmer-Scholle, 2006). Aragonite is very unstable in meteoric water (e.g., Land, 1967) and at higher temperatures (e.g., Melim et al., 2001), making it prone to dissolution. Once exposed to meteoric water, aragonite can begin to dissolve within a short time (hundreds of years) (e.g., Land, 1967, 1970; Loucks and Patty, 2017). This dissolution produces not only moldic pores but also large quantities of calcium carbonate that may be precipitated as cement around grains, forming a rigid framework that impedes compaction (Fig. 4C). Therefore, this early cementation inhibits compaction but also occludes some of the primary interparticle as well as intraparticle pores (e.g., grain bodies or living voids) and newly created moldic pores (Loucks and Patty, 2017). The resulting pore network of aragonite grain-dominated sands and gravels is a mixture of primary interparticle pores and secondary moldic pores (Fig. 4C). The effective pore network will depend on the abundance of primary pores, as moldic pores are commonly not well connected to the interparticle pore system (e.g., Lucia, 1995). In some cases, aragonite ooid sands lithify into lime grainstones with abundant moldic pores (Fig. 4C) and few, if any, interparticle pores, producing a porous grainstone with extremely poor permeability (e.g., Loucks and Patty, 2017).

### Mg–Calcite Grain-Dominated Mineralogy

Mg–calcite grains are also common in the Lower Cretaceous throughout the Gulf of Mexico and include red algae, benthic foraminifers (especially larger foraminifers), stromatoporoids, bryozoans, and echinoderms echinoderms (e.g., Flügel, 2004; Scholle and Ulmer-Scholle, 2006). The microbial encruster *Lithocodium* was also composed of Mg–calcite, as were some ooids. Similar to aragonite, Mg–calcite is very unstable in meteoric water and with burial to higher temperatures (e.g., Land, 1967, 1970; Loucks et al., 2013; Loucks and Patty, 2017). Loucks et al. (2013) has shown that as Mg–calcite undergoes diagenesis, it converts to microrhombic calcite with abundant micropores between the microrhombs (Figs. 4D and 4E). These abundant micropores may contribute to porosity but do not significantly affect permeability. Micropores are important because they exist to deeper burial depths than do macropores (Loucks et al., 2013; Brown, 2015). This concept is addressed later in the section on case studies.

### Dolomite Replacement

Dolomitization is a diagenetic process that has many origins (see Machel [2004] for a review). It generally does not create porosity but does preserve inherited pores from the limestone. Many of the Lower Cretaceous carbonates in the Gulf of Mexico contain some dolomite; however, as the database in this investigation shows, dolomite reservoirs are not as common as limestone reservoirs. The process of dolomitization may only partly replace the limestone, which has little effect on the final pore network, or it may be so extensive that it produces a very low-permeability dolostone. Where dolomitization has preserved inherited pores, the original grains and pore types also may be preserved; or dolomitization may have been so intense that all grains are masked and the pores now appear as intercrystalline pores. Overdolomitization (extensive dolomitization where porosity is nearly or completely occluded [Halley and Schmoker, 1983]) can occlude much of the pore space (Fig. 4F).

## OVERVIEW OF NORTHERN GULF OF MEXICO RIM RESERVOIR-QUALITY STATISTICS

### Description of Core-Plug Porosity and Permeability Database

As mentioned earlier, over 21,000 core-plug porosity and permeability data points have been assembled into a digital database. Each core-plug porosity and permeability data point includes calculated temperature and pressure data, making the database an invaluable tool for evaluating the effects of burial on reservoir quality. Depth values do not reflect a direct relationship with porosity and permeability, whereas temperature and pressure do have a direct effect on diagenesis and must be considered for reservoir-quality prediction. Previous studies by Loucks et al. (1984) and Dutton et al. (2012) have shown that temperature has a strong relationship to porosity and permeability and is the best parameter with which to compare values from different areas, especially where geothermal gradients vary. Loucks et al. (1984) have shown in Tertiary sandstone that pressure has little effect on reservoir quality after the sediments become cemented by a rigid cement framework. Therefore, in the analysis of porosity and permeability in this present investigation, temperature will generally be used to compare reservoir-quality burial trends.

Several pitfalls related to how data are recorded, collected, and analyzed must be recognized when using databases such as the one in this study. Temperature and pressure are dependent on the accuracy of the data recorded on log headers. Also, pressure is derived from mud weight, which can vary by drilling requirements and by operator. Even if the temperature and pressure are accurate under present-day conditions, the burial history of the formation of interest needs to be understood because the formation may have experienced higher temperatures and pressures in the past during deeper burial. Even with these possible limitations to the accuracy of individual data points, a large dataset such as the one that forms this investigation appears to be robust enough that general trends and concepts can be developed.

### Environmental Condition of Assembled Data

Core data were collected in a wide area spanning from the Texas-Mexico border to southern Florida (Fig. 1). As noted in Figure 5, sample depths range from 2000 ft (610 m) to nearly 20,000 ft (6100 m). Temperatures are between 100ºF (38ºC) and 450ºF (232ºC) (Fig. 5A), and pressures are between 850 psi and 15,750 psi (Fig. 5B). At some depths, temperatures for samples can vary by 90ºF (32ºC) (Fig. 5A) and pressures by 6000 psi (Fig. 5B). In general, the lower thermal gradients are in zones 5 and 6, and the higher thermal gradients are in zones 1 and 2.

Some results do not fit the general trend, such as some of the zone 4 samples that cluster at anomalously high temperatures at a given depth (Fig. 5A). These hotter zones are in the Pettet Limestone in Caddo Parish, Louisiana. Also, many of the samples that are buried at greater than 13,000 ft (3962 m) are from overpressured zones (Fig. 5B). These contrasting values at similar depths serve as a precautionary warning: when predicting porosity and permeability at depth, one must understand the environmental conditions of the target zone.

### Porosity Versus Permeability Analysis

The regression plot of porosity versus permeability (Fig. 6) shows a fair relationship between the two variables (coefficient of determination [$R^2$] = 0.63). Relative to each porosity unit are

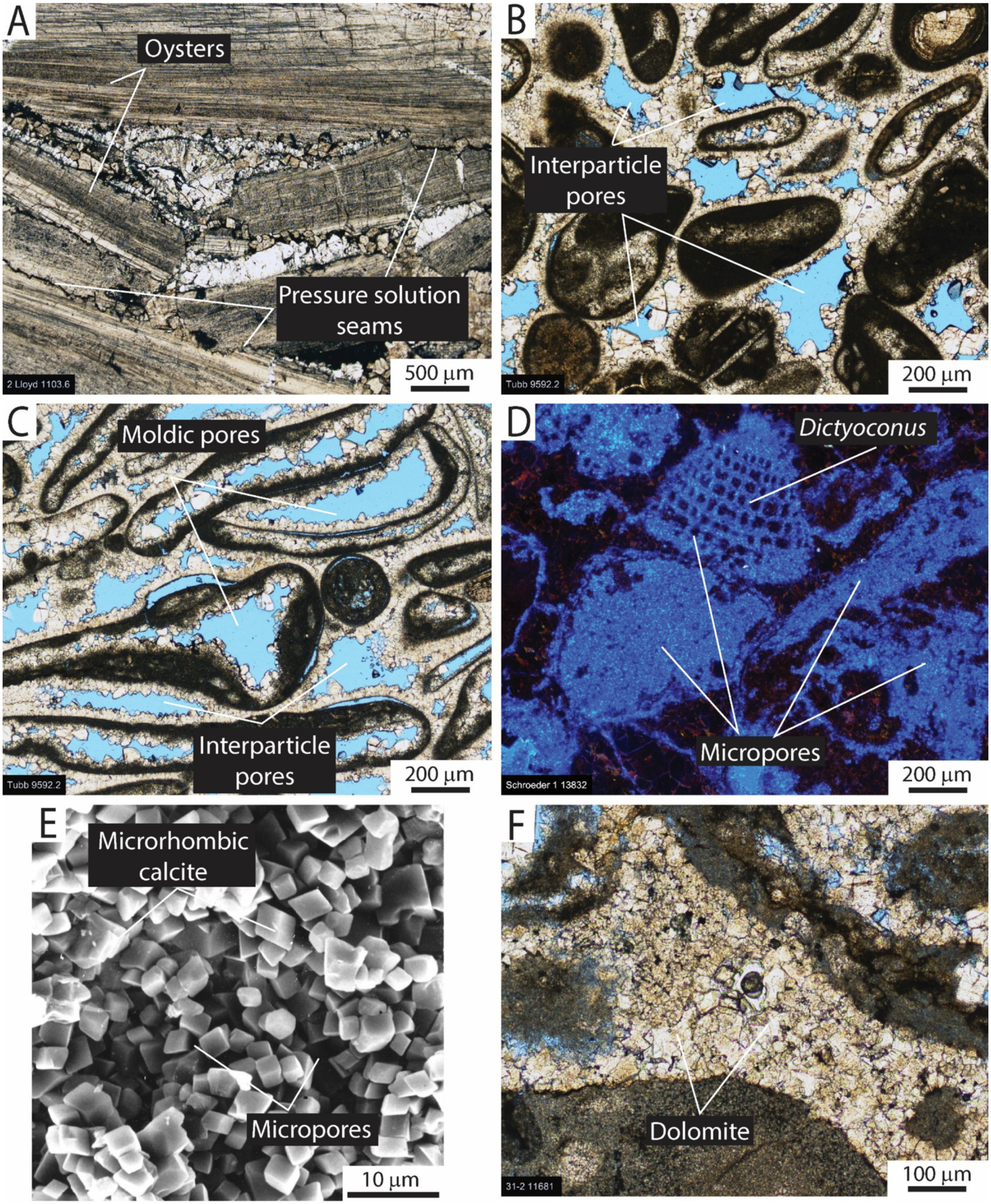


generally three orders of magnitude of permeability associated with that porosity value. Permeability values of 0.05 md and less appear to fit a straight line relative to porosity, which is probably related to the inability of standard core analysis to accurately measure permeability with older equipment. The values in the upper left portion of the graph circled in red are thought to be fractured core-plug samples that provided anomalously high permeability values for lower porosity samples. The area circled in

**(FACING PAGE) Figure 4. Diagenesis and pore types associated with different initial carbonate sediments. (A) Calcite-rich grains composed of oyster fragments show extensive compaction as evidence of pressure-solution seams and loss of primary interparticle pores. James Limestone, Sun Oil 2 Lloyd (9103.6 ft [2774.80 m]), Henderson County, Texas. (B) Highly micritized grains with rigid rim of bladed calcite. Interparticle pores are well preserved. Glen Rose Limestone, Lasmo 1 Tubb (9592.2 ft [2923.7 m]), Henderson County, Texas. (C) Mollusk grainstone originally composed of aragonitic bivalves. Mg–calcite micrite envelopes formed around the bivalves; later, the aragonite bivalves dissolved, forming moldic pores. Early calcite cement formed a rigid framework that inhibited compaction, and allowed preservation of primary pores. Glen Rose Limestone, Lasmo 1 Tubb (9592.2 ft [2923.7 m]), Henderson County, Texas. (D) Micropores within former Mg–calcite foraminifers (*Dictyoconus*), as shown by the blue areas, where blue fluorescent dye impregnated the thin-section stub. Stuart City Limestone, Pioneer Energy 1 Schroeder (13,832 ft [42160 m]), Bee County, Texas. (E) SEM image of microrhombic calcite and associated micropores in a transformed Mg–calcite grain. Calvin Limestone, ARCO 1 Huffman McNeely, Natchitoches Parish, Louisiana. (F) Interparticle pore space filled with dolomite cement occluding most of the pore. Sunniland Limestone, Sun Oil 31–2 Red Cattle (11,681 ft [3560.4 m]), Henry County, Florida.**

red in the lower center of the graph is generally where high porosity samples contain abundant micropores and have very low permeabilities. These also could be samples that have oomoldic pores but no interparticle pores.

This porosity versus permeability graph (Fig. 6) is interesting as an overview of the range in porosity and permeability in the Lower Cretaceous carbonates in the northern rim of the Gulf of Mexico, but it is not of use as an aid in defining risk factors for reservoir quality in a given area. The best use of these data in calculating a risk factor is to analyze data in the local area of interest, in a similar formation, and at the predicted temperature of the prospect. Figure 7 shows porosity versus permeability by zones along the northern rim of the Gulf of Mexico.

## Reservoir-Quality Trends with Depth and Temperature

Figure 8 displays plots of porosity and permeability versus depth and temperature for all the data, and Figures 9 and 10 show similar plots for the different geographic zones. It is emphasized that temperature is a better parameter than depth for comparison with porosity and permeability. Depth is not a definitive term in the sense of factors controlling porosity and permeability. As documented by Dutton et al. (2012), temperature is the most useful parameter to use to understand changes in porosity and permeability with burial and to use to compare data from areas with different geothermal gradients.

Porosity decreases with increasing depth and temperature (Figs. 8A and 8B); however, the trends are not simple. What is noted is that maximum porosity does decrease with depth, as does the range of porosity values. Very low porosity values (less than 2%), present at most depths, are commonly related to textures such as mudstones and wackestones (rocks with abundant matrix) (e.g., Loucks, 2002). Schmoker and Halley (1982) also documented a general decrease in porosity with depth (surface to 18,000 ft [5486 m]) in Lower Cretaceous carbonates in Florida using borehole logs; no rock data were used.

It is suggested that a porosity versus temperature plot be used for plotting porosity with burial. In comparing the porosity versus temperature and porosity versus depth graphs, one can see that the distribution of data has shifted. As an example, porosity data from zone 1 at approximately 17,000 ft (5182 m) and porosity data from zone 2 at 19,000 ft (5791 m) plot in a similar temperature range (430ºF [221ºC]) in the porosity versus temperature graph (Figs. 8A and 8B).

Trends seen in the porosity versus depth and permeability versus depth plots are similarly noted in the porosity versus temperature and permeability versus temperature plots (Figs. 8C and 8D). Permeability decreases with depth and temperature. In the permeability versus temperature plot (Fig. 8D), there is a sharp change at approximately 275ºF (135ºC) from permeability values primarily greater than 100 md to permeability values less than 10 md. This sharp change is related in part to variable permeability related to dominant lithologies in different formations, such as higher permeability values in the Pettet grainstones where the strata is dominated by interparticle and moldic macropores as compared to lower permeability values in the Stuart City and Sligo platform-edge boundstones, dominated by micropores. Also, higher temperatures in the deeper buried Stuart City and Sligo limestones had a role in reducing permeability by promoting cementation of macropores.

# SELECTED CASE STUDIES

## Introduction to Case Studies

Numerous case studies in the literature have investigated pore networks in Lower Cretaceous strata along the onshore northern rim of the Gulf of Mexico. This section presents several case studies where both thin sections and core-plug data are available. The selected case studies cover a range of ages, depositional settings, and original mineralogies that present a spectrum of carbonate pore networks and associated reservoir quality in the Lower Cretaceous northern Gulf of Mexico stratigraphic section.

## Micropore-Dominated Pore-Network Case Studies

### Valanginian Calvin Limestone Shelf-Margin Reef Complex in Louisiana

The Valanginian Calvin Limestone is a deeply buried carbonate shelf-margin system that has been identified in East Texas and Louisiana (Loucks et al., 2017) (Figs. 1 and 2). Where drilled, it is as thick as 2000 ft (610 m) and the lithofacies are composed of backreef, reef, and forereef strata. The shelf margin produced a prominent reef complex with a margin-to-lagoon relief of 200 to 500 ft (61 to 152 m) and a shelf-to-basin relief of approximately 1000 ft (305 m). Core-plug data (15,499 to 17,480 ft [5328 m to 7424 m]) from the ARCO 1 Huffman McNeely well in Natchitoches Parish, Louisiana, are shown in Figure 11A. The pore network is dominated by micropores (Figs. 12A–12C) and the unit has a mean porosity of 3.6% (range from 1.2 to 8.9%), mean permeability of 0.11 md (range from <0.01 to 0.73 md), and geometric mean permeability of 0.03 md. These values are common for deeply buried micropore networks (Loucks et al., 2013). Micropores were developed by the diagenesis of former Mg–calcite grains such as *Lithocodium* (Fig. 12A), stromatoporoids, and peloids to calcite. The micropores occur between microrhombic crystals of calcite (Figs. 4E and 12C). Therefore, this reservoir has low quality related to dominantly micropores but it would be a candidate for gas production where charged.

### Barremian Sligo Limestone Shelf-Margin Reef Complex in South Texas

The Barremian Sligo reef-margin reef complex is a deep gas producer in South Texas (Bebout et al., 1981; Kirkland et al.,

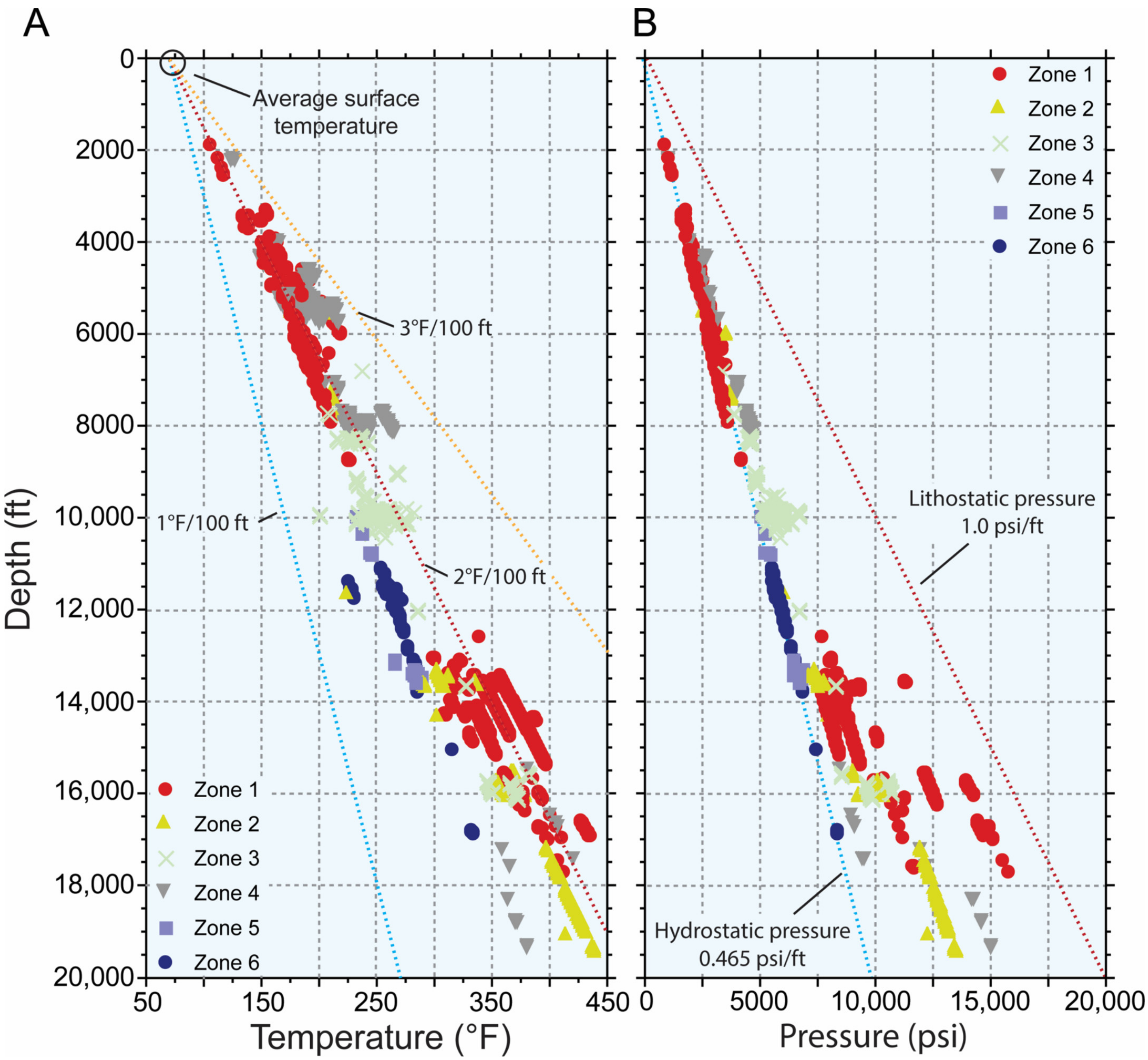


**Figure 5. Environmental conditions of porosity and permeability samples. Data points color coded by geographic zones displayed in Figure 1. (A) Temperature versus depth. Note that zones 1–3 generally show a higher geothermal gradient than zones 4–6. (B) Pressure versus depth. 2000 ft = 610 m; 50–450°F = 10–232°C; 1°F = 1.82°C/100 m; 5000 psi = 34.5 MPa; and 1 psi/ft = 22.6 kPa/m.**

1987) (Figs. 1 and 2). At the shelf margin, the section is greater than 1000 ft (305 m) thick, and reservoir lithofacies range from back-reef coral-caprinid grainstones to reefal coralgal boundstones. The pore network is dominated by micropores associated with *Lithocodium* and larger foraminifers. The interparticle, intraparticle, and moldic macropores are occluded with calcite cement. Mean porosity of this unit is 3.9% (range from 0.1 to 15.1%), mean permeability is 0.23 md (range from <0.01 to 15.4 md), and geometric mean permeability is 0.04 md. A plot of porosity versus permeability is shown in Figure 11B. The majority of permeability values are less than 1 md, which is common for deeply buried microporous strata. In Figure 11B, the higher permeability values (greater than approximately 5 md) associated with porosities less than 10% may be related to fractured core-plug samples. The micropore network in the deep Sligo reef trend allows for the production of gas.

### Aptian James Limestone of the Pearsall Formation in Poplarville Field Area, Southwestern Mississippi

The Aptian James Limestone in the Poplarville Field is composed of a shoaling complex of hydrozoa/cryptalgal stromatolite bindstones and requienid/coral packstones, grainstones, and boundstones (Loucks et al., 1996) (Figs. 1 and 2). The shoaling complex developed over deeper buried salt-dome structures. At these burial depths of greater than 14,000 ft (4270 m) reservoir quality is relatively poor (Fig. 11C). Most of the macropores are cemented. Micropores are dominant and are associated with

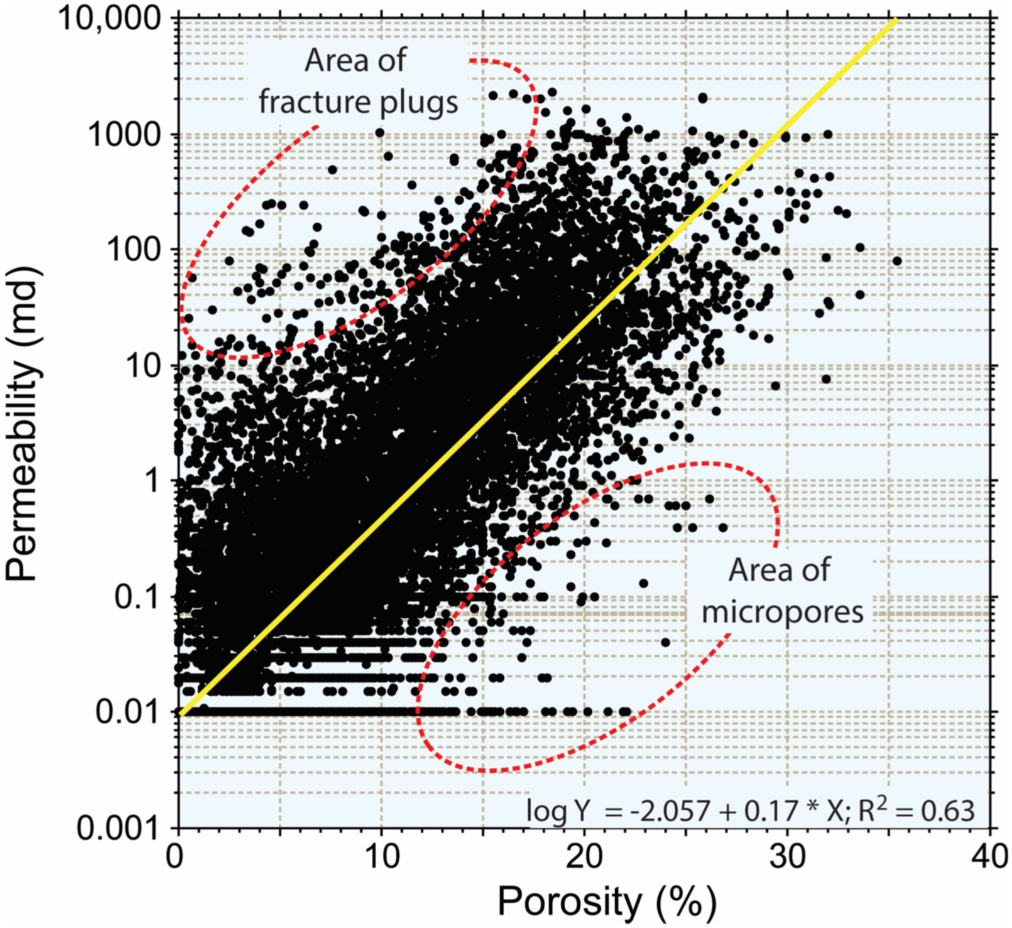


**Figure 6. Porosity versus permeability plot for all data. Best-fit regression line provided in yellow. $R^2$ = 0.63. Possible fracture plugs circled in red in upper left, and area of micropores circled in red in lower center.**

cryptalgal stromatolite bindstones (microbialites). The major binding organism is *Lithocodium*. Mean porosity is 4.3% (range from 0.9 to 16.7%), mean permeability is 0.12 md (range from <0.01 to 4.0 md), and geometric mean permeability is 0.005 md. The micropore-dominated reservoir in the Poplarville Field is a gas producer.

### Albian Stuart City Limestone Shelf-Margin Reef Complex in South Texas

The Aptian Stuart City reef trend is a major reef system in the Lower Cretaceous in South Texas (Bebout and Loucks, 1974; Phelps et al., 2013; Waite, 2009) (Figs. 1 and 2). The reef complex is over 1200 ft thick and there is up to 300 ft (91 m) of relief between the landward shelf and the reef-complex top. As with the Sligo reef trend, the Stuart City reef complex is composed of lithofacies ranging from back-reef coralgal-caprinid grainstones and reefal coralgal rudist boundstones. *Lithocodium* is a major component that binds the boundstones. The porosity and permeability plots show poor to fair reservoir quality (Fig. 11D). Most of the pores are micropores (Fig. 12F) associated with *Lithocodium* and larger foraminifers (Figs. 12D and 12E) that had an original mineralogy of Mg–calcite (Loucks et al., 2013). The interparticle macropores between grains and the intraparticle and moldic macropores associated with former aragonite rudists are generally well cemented with calcite. The porosity versus permeability plot (Fig. 11D) shows a mean porosity of 4.6% (range from <0.01 to 19.9%), mean permeability of 0.31 md (range from <0.01 to 17.0 md), and geometric mean permeability of 0.06 md. The Stuart City reservoirs have been well-developed as tight-carbonate reservoirs over the past 15 yr, which is related mostly to advances in horizontal drilling and completion technology and high average natural gas prices prior to the end of 2008 (Loucks et al., 2013).

## Macropore-Dominated Pore-Network Case Studies

### Barremian Sligo/Pettet Limestone Platform Deposits in Northwestern Louisiana

The Barremian Pettet Limestone in Caddo Parish, Louisiana, contains skeletal- and ooid-rich grainstones that have good to excellent reservoir quality (Fig. 13A) and have been prolific producers of hydrocarbons (Howard, 1950; Mitchell-Tapping, 1981). The porosity versus permeability plot (Fig. 13A) shows a mean porosity of 9.6% (range from 0.01 to 32.1%), mean permeability of 6.2 md (range from <0.01 to 428 md), and geometric mean permeability of 0.18 md. Mitchell-Tapping (1981) noted that the ooid grainstones have excellent interparticle pores as well as moldic and micropores. The ooids appear to have been radial Mg–calcite, which is prone to form micropores (Loucks et al., 2013).

### Aptian James Limestone of the Pearsall Formation in Fairway Field Area, East Texas Basin

The Aptian James Limestone in the Fairway Field is composed of a patch-reef complex that developed over mobile salt domes (Terriere, 1976; Achauer, 1985; Webster et al., 2008; Hattori et al., 2019). Associated with the patch reefs are reef-talus grainstones with very good reservoir quality (Hattori et al., in preparation) (Fig. 13B). The porosity versus permeability plot (Fig. 13B) shows a mean porosity of 8.8% (range from 0.01 to 26.7%), mean permeability of 16.8 md (range from <0.01 to 900

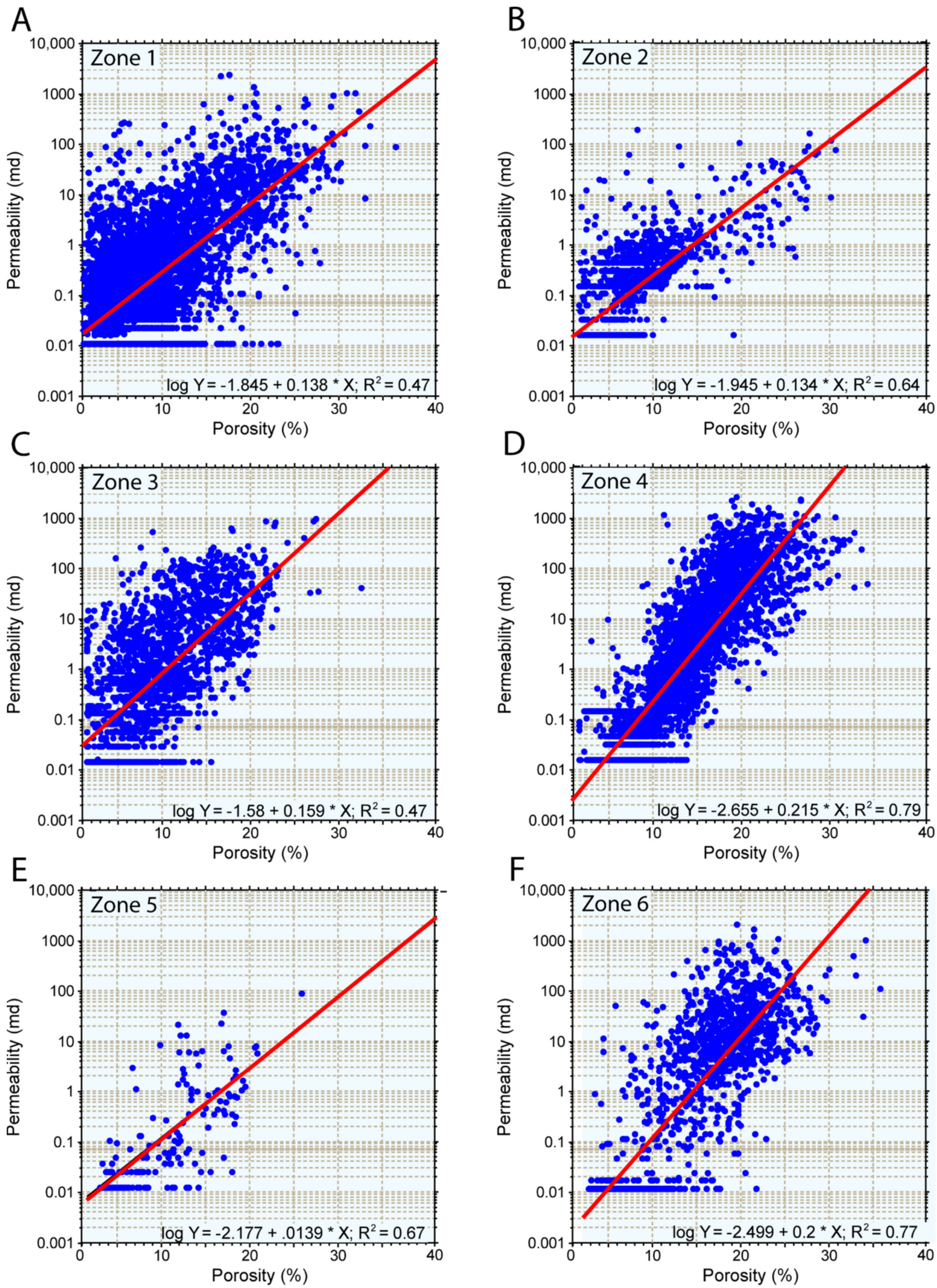
A
Zone 1
log Y = -1.845 + 0.138 * X; R² = 0.47
B
Zone 2
log Y = -1.945 + 0.134 * X; R² = 0.64
C
Zone 3
log Y = -1.58 + 0.159 * X; R² = 0.47
D
Zone 4
log Y = -2.655 + 0.215 * X; R² = 0.79
E
Zone 5
log Y = -2.177 + .0139 * X; R² = 0.67
F
Zone 6
log Y = -2.499 + 0.2 * X; R² = 0.77
Permeability (md)
Porosity (%)
10,000
1000
100
10
1
0.1
0.01
0.001
0
10
20
30
40

**(FACING PAGE) Figure 7. Porosity versus permeability plots by geographic zone. (A) Zone 1: Has fair $R^2$. Abundant low reservoir-quality data from the deep Sligo and Stuart City shelf-margin reef trends. (B) Zone 2: Has fair $R^2$. (C) Zone 3: Has fair $R^2$. Abundant high reservoir-quality data from the Pettet Limestone. (D) Zone 4: Has good $R^2$. Abundant high-quality data from the Pettet Limestone. (E) Zone 5: Has fair $R^2$. Data mainly from Waveland Field in Mississippi. (F) Zone 6: Has good $R^2$. Data from Sunniland Limestone in South Florida.**

md), and geometric mean permeability of 0.88 md. The strata contain good interparticle pores along with moldic pores and micropores within grains (Fig. 14A and 14B). The James reservoirs in the Fairway Field have a long history of production from this macropore-dominated section.

### Aptian Cow Creek and Bexar Limestones of the Pearsall Formation on the Pearsall Arch, South Texas Shelf

The Cow Creek and Bexar members of the Aptian Pearsall Formation were deposited in a shoal-water carbonate complex on the Pearsall Arch (Loucks, 1977). The higher energy strata are composed mainly of echinoid-oyster grainstones and a few microbialite bound patch reefs. The grainstones and some packstones contain good interparticle pores and abundant moldic pores. The moldic pores are associated with former aragonite bivalve grains. The calcite oyster fragments did not dissolve and helped form a rigid framework. Mean porosity is 13.4% (range from 1.4 to 30.9%), mean permeability is 22.8 md (range from <0.01 to 960 md), and geometric mean permeability is 1.3 md (Fig. 13C). These high-quality Cow Creek and Bexar macropore reservoirs are not producing in South Texas as they appear not to have an updip seal (Loucks, 1977).

### Albian Sunniland Limestone on the Western Florida Shelf

The Albian Sunniland Limestone is the major producer in South Florida (e.g., Mitchell-Tapping, 1984, 2003). It was deposited on a moderate to high-energy shelf approximately 200 mi behind the shelf-margin reef. The producing porous strata are grainstones and some boundstones that reflect a higher energy shoaling system. Good interparticle pores developed along with moldic pores (Fig. 14C). Some of the strata are dolomitized and provide some high permeability zones (Fig. 14D). The porosity versus permeability plot (Fig. 13D) shows a mean porosity of 10.0% (range from 0.4 to 33.6%), mean permeability of 25.5 md (range from <0.01 to 2000 md), and geometric mean permeability of 0.28 md. These high reservoir-quality values at depths of 11,500 to 13,000 ft are in part related to a generally lower thermal gradient (approximately 1.6ºF/100 ft [2.92ºC/100 m]) and in some cases dolomitization with the development of abundant intercrystalline pores. The Sunniland Field has been an excellent producer from high-quality macropore reservoirs.

### Albian Glen Rose Limestone in the Alabama Ferry Field, Houston Trough, East Texas

The mollusk-ooid grainstones in the Glen Rose Formation in the Alabama Ferry Field area have been previously interpreted as an ooid shoal complex (e.g., Fitchen et al., 1997; Zahm, 2010); however, a recent reinterpretation by Soto-Kerans et al. (2017) proposed that the grainstone bodies are composed of resedimented allochems transported from the adjacent shelf into a dysaerobic intraplatform basin. This reinterpretation is based on the absence of cross-bedding in the ooid-bearing grainstone bodies, a mixed allochem assemblage uncommon to shoals, and interbedded organic-rich argillaceous mudstones. Soto-Kerans et al. (2017) also mapped out an intraplatform basin where the Alabama Ferry Field lies. The major pore types are interparticle and moldic (Figs. 14E and 14F). Moldic pores are very common in the thin, fragmented bivalve shells. The porosity and permeability plots show poor to good reservoir rock (Fig. 13E). The porosity versus permeability plot (Fig. 13E) indicates a mean porosity of 6.0% (range from 0.01 to 32.0%), mean permeability of 7.2 md (range from <0.01 to 130 md), and geometric mean permeability of 0.22 md. Many of the moderately buried Lower Cretaceous grainstones in the onshore Gulf of Mexico have a similar macropore reservoir type as these Glen Rose grainstones.

## DISCUSSION

The large core-plug porosity and permeability database constructed for this investigation has value in developing concepts for reservoir-quality risk analysis. These data show what has actually been found and measured and at what depths and temperatures they occur (Fig. 3). If values higher than those presented in the graphs constructed from the database are predicted, then some sound scientific explanation is necessary to substantiate the prediction. It should be noted that it is best to use data as close to the area of interest as possible, as well as data from the same geologic unit because this database contains such a large selection of data across a broad spectrum of locations, formations, depths, and temperatures.

The different reservoir-quality plots show trends of maximum values generally decreasing with increased depth and temperature (Figs. 8–10). The maximum values are important because they provide an upper limit of magnitude; however, the full range of values at any depth interval needs to be considered while calculating a reservoir-quality risk factor. Statistically, the mean value should be considered as the most logical estimation of reservoir quality unless reservoir quality has been separated by lithofacies. Then, the chance of encountering the higher reservoir-quality lithofacies becomes an important factor in determining risk.

An important concept stressed in this investigation is that temperature and not depth should be used as the measure of comparison if using data from a distant area to estimate reservoir quality in the area of interest. Areas of different geothermal gradients can produce dissimilar reservoir quality within the same lithofacies because degrees of diagenesis are strongly controlled by temperature. Also, caution should be taken within areas that had a complex burial history, as the strata would probably have experienced higher temperatures and pressures at maximum burial.

As noted throughout this investigation, initial mineralogy, diagenetic pathway, and depth of burial (thermal exposure) have a strong control on the development of pore networks. It is important to obtain as much knowledge about original mineralogy as possible to estimate what types of pores may have developed. Obviously, the diagenetic pathway of the strata and thermal history must also be taken into consideration.

This investigation includes nine case studies from well-studied reservoirs to demonstrate the variation in reservoir quality that can occur as a result of variable original mineralogy, pore network type, diagenesis, and burial history (Figs. 11 and 13). In the nine case histories presented, four are dominated by micropores, and the other five by macropores with lesser micropores (Fig. 15). It is important to note that micropores are an extremely common pore type but are commonly overlooked because of their small size, especially reservoirs dominated by macropores (Loucks et al., 2013). Special analysis—such as blue fluorescent dye, SEM, or high-pressure mercury injection capillary pressure (MICP)—may be necessary to recognize and quan-

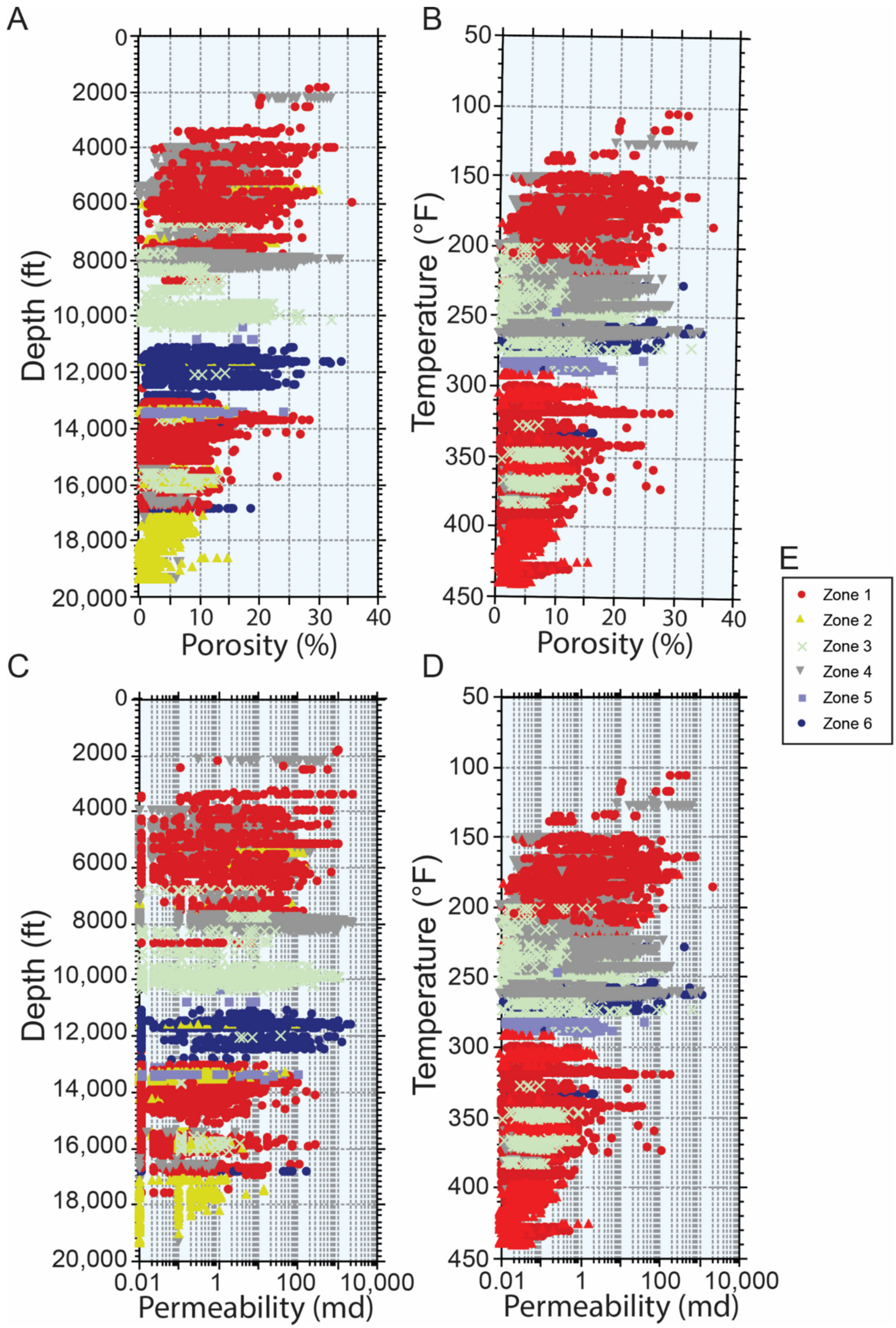

A
Depth (ft)
0
2000
4000
6000
8000
10,000
12,000
14,000
16,000
18,000
20,000
0
10
20
30
40
Porosity (%)
B
Temperature (°F)
50
100
150
200
250
300
350
400
450
0
10
20
30
40
Porosity (%)
C
Depth (ft)
0
2000
4000
6000
8000
10,000
12,000
14,000
16,000
18,000
20,000
0.01
1
100
10,000
Permeability (md)
D
Temperature (°F)
50
100
150
200
250
300
350
400
450
0.01
1
100
10,000
Permeability (md)
E
Zone 1
Zone 2
Zone 3
Zone 4
Zone 5
Zone 6

**(FACING PAGE) Figure 8. Porosity and permeability versus depth and temperature. All data points color coded by geographic zone. (A) Porosity versus depth. (B) Porosity versus temperature. (C) Permeability versus depth. (D) Permeability versus temperature. (E) Code for zone symbols.**

tify micropores. However, micropores should not be undervalued as they are the last pore type to be occluded with burial (Loucks et al,. 2013; Brown, 2015) and are therefore important in deeply buried formations, such as those in the micropore-dominated case histories reported in this study (depth greater than 12,000 ft [3658 m]).

It is interesting to compare the case histories dominated by macropores versus micropores. Figure 15 presents a graph that plots mean porosity versus geometric mean permeability for each of the nine case studies described in this investigation. The micropore-dominated pore networks all plot in the area of less than 5% mean porosity and less than 0.1 md geometric mean permeability. The macropore-dominated pore networks all plot in the area greater than 5% mean porosity and greater than 0.1 md geometric mean permeability. Another concept presented by Figure 15 is that even the reservoirs with macropore-dominated pore networks have relatively low geometric mean permeability (less than 2 md), which reiterates that the higher permeability values in a dataset of a particular unit must be understood relative to their origin—such as lithofacies, texture, and mineralogy—to best predict how to risk economic porosity and permeability.

Statistical datasets are important for ground-truthing wireline-log calculated porosity and permeability values. If wireline-log calculations provide higher values for porosity than have been documented by actual data, then the calculation should be questioned. The statistical data can also help develop algorithms for estimating permeability from calculated wireline-log porosity values. The permeabilities from the statistical data will reflect the effect of pore types on permeability.

## CONCLUSIONS

The construction of large statistical core-plug porosity and permeability databases is valuable for understanding and improving the calculation of reservoir-quality risk factors for carbonate plays. The porosity and permeability database developed in this investigation for the onshore northern rim of the Gulf of Mexico demonstrates that a number of concepts can be derived from having a large volume of porosity and permeability values and associated parameters such as depth, temperature, and pressure. Also, the integration of pore-type observations with the porosity and permeability measurements provides insight into reservoir-quality values that are associated with different pore networks. Rock parameters such as lithofacies, textures, mineralogy, etc. must be considered when predicting probable pore networks and diagenetic processes.

A spectrum of case histories of reservoir quality in reservoirs from the northern rim of the Gulf of Mexico suggests that there are two main reservoir types: those associated with dominantly macropore-network systems and those associated with dominantly micropore-network systems. Macropore systems are generally associated with shallower reservoirs (less than 12,000 ft [3660 km]), and micropore systems with deeper reservoirs (greater than 12,000 ft [3660 km]) because macropores are commonly occluded with increased burial, leaving only micropore-dominated pore networks at greater depths.

The statistical plots derived from the database can be used as guidelines to estimate expected reservoir quality at a given depth or temperature. Temperature is considered a better parameter to use because it has a direct control on diagenesis and, thus, reservoir quality, whereas depth may not be representative of the full burial history of the reservoir formation. If estimated reservoir-quality values for a given play are higher than those provided by the database, then a sound scientific reason must be postulated. Also, if calculated wireline-log porosity and permeability appear high relative to the database, further investigation is needed to check if the calculations are correct.

Large statistical reservoir-quality databases are valuable for understanding and calculating risk factors and should be constructed for other areas where abundant core-plug data are available. To develop the highest-quality databases, it is best to take thin-section stubs from core plugs in order to define lithofacies, mineralogy, pore types, and, if possible, high-pressure MICP analysis for measuring pore-throat sizes.

## ACKNOWLEDGMENTS

We want to recognize the Carbonate Reservoir Characterization Research Laboratory (RCRL) at the Bureau of Economic Geology (Bureau) and associated sponsors for support of this investigation. Joseph Su of the Bureau helped in constructing the interactive reservoir-quality database. Patrick Smith of the Bureau helped with the SEM images. I appreciate the reviews of the manuscript by Chandier Wilhelm, Kelly Hattori, James Willis, and an anonymous reviewer.

Stephanie Jones of the Bureau edited the manuscript, and I recognize her effort. Publication authorized by the Director, Bureau of Economic Geology, Jackson School of Geosciences, University of Texas at Austin.

## REFERENCES CITED

Achauer, C. W, 1985, Facies, morphology, and major reservoir controls in the Lower Cretaceous James Reef, Fairway Field, East Texas, *in* P. O. Roehl and P. W. Choquette, eds., Carbonate petroleum reservoirs: Springer-Verlag, New York, p. 485–494.

Bebout, D. G., D. A. Budd, and R. A. Schatzinger, 1981, Depositional and diagenetic history of the Sligo and Hosston formations (Lower Cretaceous) in South Texas: Bureau of Economic Geology Report of Investigations 109, Austin, Texas, 69 p.

Bebout, D. G., and R. G. Loucks, 1974, Stuart City Trend (Lower Cretaceous, South Texas: A carbonate shelf-margin model for hydrocarbon exploration: Bureau of Economic Geology Report of Investigations 78, Austin, Texas, 80 p.

Brown, A. A., 2015, Surface energy effects on formation and preservation of microrhombic calcite fabrics and porosity: American Association of Petroleum Geologists Search and Discovery Article 51148, Tulsa, Oklahoma, 25 p., <http://www.searchanddiscovery.com/pdfz/documents/2015/51148brown/ndx_brown.pdf.html>.

Choquette, P. W., and L. C. Pray, 1970, Geological nomenclature and classification of porosity in sedimentary carbonates: American Association of Petroleum Geologists Bulletin, v. 54, p. 207–250.

Corrigan, J, 2003, Correcting bottom hole temperature data: ZetaWare, Utilities—BHT correction home page, <http://zetaware.com/utilities/bht/timesince.html>.

Drilling Formulas and Drilling Calculations, 2018, <http://www.drillingformulas.com/about-drillingformulas-com>.

Dunham, R. J., 1962, Classification of carbonate rocks according to depositional texture, *in* W. E. Ham, ed., Classification of carbonate rocks: American Association of Petroleum Geologists Memoir 1, Tulsa, Oklahoma, p. 108–121.

Dutton, S. P., R. G. Loucks, and R. J. Day-Stirrat, 2012, Impact of regional variation in detrital mineral composition on reservoir quality in deep to ultradeep lower Miocene sandstones, western Gulf of Mexico: Marine and Petroleum Geology, v. 35, p. 139–153, <https://doi.org/10.1016/j.marpetgeo.2012.01.006>.

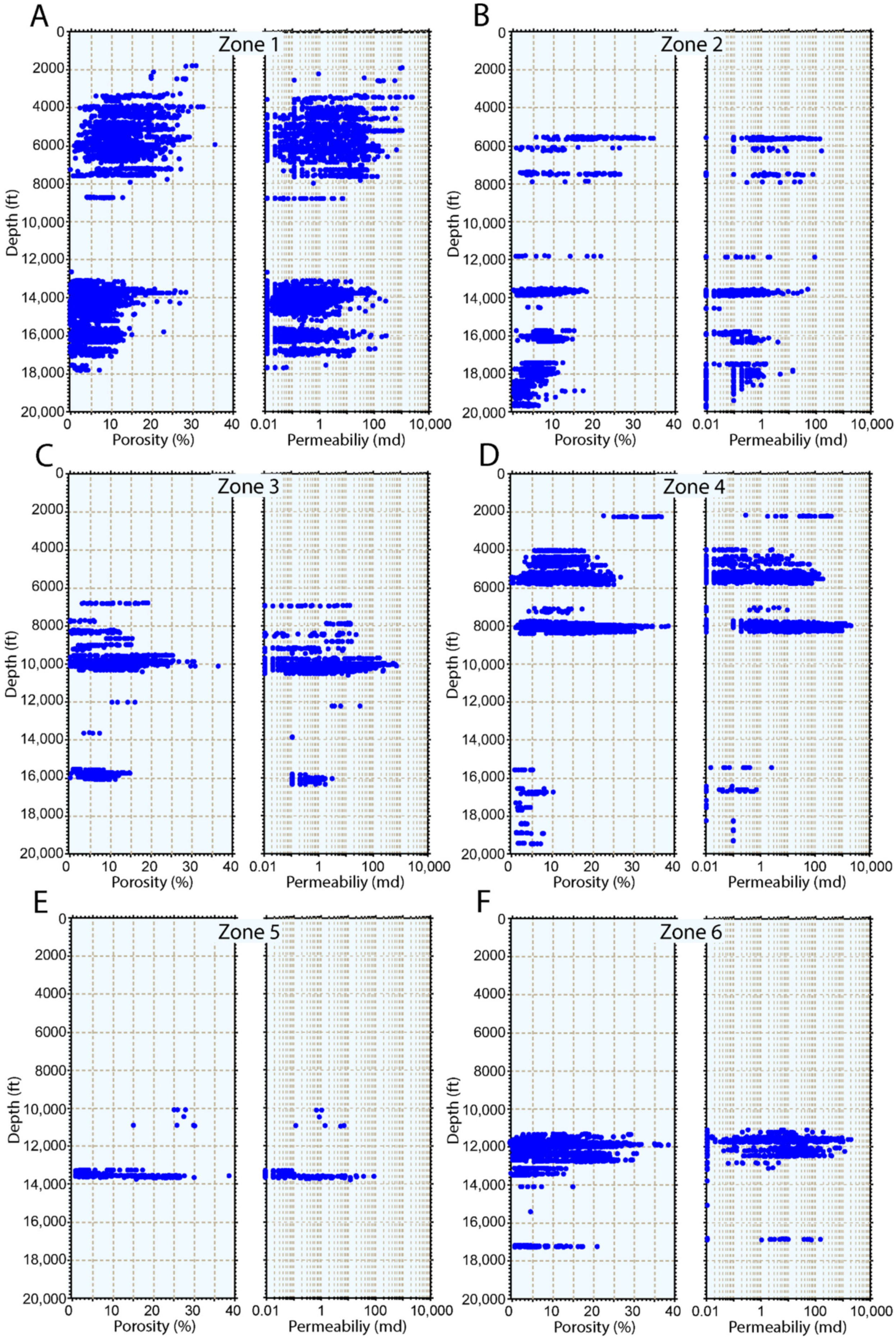
A
Zone 1
B
Zone 2
C
Zone 3
D
Zone 4
E
Zone 5
F
Zone 6
Depth (ft)
0
2000
4000
6000
8000
10,000
12,000
14,000
16,000
18,000
20,000
Porosity (%)
0 10 20 30 40
Permeabiliy (md)
0.01 1 100 10,000

**(FACING PAGE) Figure 9. Porosity and permeability versus depth by geographic zone. (A) Zone 1. (B) Zone 2. (C) Zone 3. (D) Zone 4. (E) Zone 5. (F) Zone 6.**


Ewing, T. E., 2003, Review of the tectonic history of the lower Rio Grande border region, South Texas and Mexico, and implications for hydrocarbon exploration, *in* N. C. Rosen, ed., Structure and stratigraphy of South Texas and northeast Mexico: Applications to exploration: Gulf Coast Section of the Society of Economic Paleontologists and Mineralogists Foundation, Houston, Texas, and South Texas Geological Society, San Antonio, p. 7–21.

Ewing, T. E., 2009, The ups and downs of the Sabine Uplift and the northern Gulf of Mexico Basin: Jurassic basement blocks, Cretaceous thermal uplifts, and Cenozoic flexure: Gulf Coast Association of Geological Societies Transactions, v. 59, p. 253–269.

Fitchen, W. M., D. G. Bebout, and D. R. Prezbindowski, 1997, Production from Cretaceous high-permeability carbonate grainstones; Alabama Ferry, North Unit, Leon County, Texas, *in* R. P. Major, ed., Oil and gas on Texas state lands: An assessment of the resource and characterization of type reservoirs: Bureau of Economic Geology Report of Investigations 241, Austin, Texas, p. 117–126.

Flügel, E., 2004, Microfacies of carbonate rocks; analysis, interpretation, and application: Springer, Berlin, Heidelberg, New York, 976 p.

Forrest, J., E. Marcucci, and P. Scott, 2005, Geothermal gradients and subsurface temperatures in the northern Gulf of Mexico: Gulf Coast Association of Geological Societies Transactions, v. 55, p. 233–248.

Halley, R. B., and J. W. Schmoker, 1983, High-porosity Cenozoic carbonate rocks of South Florida: Progressive loss of porosity with depth: American Association of Petroleum Geologists Bulletin, v. 67, p. 191–200.

Hattori, K. E., R. G. Loucks, and C. Kerans, 2019, Stratal architecture of a halokinetically controlled patch reef system: A case study from the Lower Cretaceous Aptian Pearsall Formation in the Fairway Field, East Texas Basin, Texas: Sedimentary Geology, v. 387, p. 87–103.

Howard E. L., 1950, Rodessa Field Cass and Marion counties, Texas, Caddo Parish, Louisiana, and Miller County, Arkansas, *in* F. A. Herald, ed., Occurrence of oil and gas in northeast Texas: University of Texas Publication 5116, Austin, Texas, p. 334–338.

Kirkland, B. L., R. G. Lighty, R. Rezak, and T. T. Tieh, 1987, Lower Cretaceous barrier reef and outer shelf facies, Sligo Formation, South Texas: Gulf Coast Association of Geological Societies Transactions, v. 37, p. 371–382.

Land, L. S., 1967, Diagenesis of skeletal carbonates: Journal of Sedimentary Research, v. 37, p. 914–930, <https://doi.org/10.1306/74d717d5-2b21-11d7-8648000102c1865d>.

Land, L. S., 1970, Phreatic versus vadose meteoric diagenesis of limestones: Evidence from a fossil water table: Sedimentology, v. 14, p. 175–185, <https://doi.org/10.1002/9781444304510.ch15>.

Loucks, R. G., 1977, Porosity development and preservation in a high-energy, shoal-water carbonate complex—Pearsall Formation, Lower Cretaceous, South Texas, *in* D. G. Bebout and R. G. Loucks, eds., Cretaceous carbonates of Texas and New Mexico—Applications to subsurface exploration: Bureau of Economic Geology Report of Investigations 89, Austin, Texas, p. 97–126.

Loucks, R. G., M. M. Dodge, and W. E. Galloway, 1984, Regional controls on diagenesis and reservoir quality in lower Tertiary sandstones along the Texas Gulf Coast, *in* D. A. McDonald and R. C. Surdam, eds., Clastic diagenesis: American Association of Petroleum Geologists Memoir 37, Tulsa, Oklahoma, p. 15–45.

Loucks, R. G., A. Abel, and M. Ver Hoeve, 1996, Paleostructure association, lithofacies architecture, and reservoir quality of the Upper James Lime (Pearsall Fm, Lower Cretaceous) in the Poplarville Field, Pearl River Co., Mississippi: Gulf Coast Association of Geological Societies Transactions, v. 46, p. 235–248.

Loucks, R. G., 2002, Controls on reservoir quality in platform-interior limestones around the Gulf of Mexico: Example from the Lower Cretaceous Pearsall Formation in South Texas: Gulf Coast Association of Geological Societies Transactions, v. 52, p. 659–672.

Loucks, R. G., F. J. Lucia, and L. Waite, 2013, Origin and description of the micropore network within the Lower Cretaceous Stuart City Trend tight-gas limestone reservoir in Pawnee Field in South Texas: Gulf Coast Association of Geological Societies Journal, v. 2, p. 29–41, <https://www.gcags.org/Journal/2013.GCAGS.Journal/GCAGS.Journal.2013.vol2.p29-41.Loucks.et.al.pdf>.

Loucks, R. G., C. Kerans, H. Zeng, and P. A. Sullivan, 2017, Documentation and characterization of the Lower Cretaceous (Valanginian) Calvin and Winn carbonate shelves and shelf margins, onshore north-central Gulf of Mexico: American Association of Petroleum Geologists Bulletin, v. 101, p. 119–142, <https://doi.org/10.1306/06281615248>.

Loucks, R. G., and K. Patty, 2017, Vadose diagenetic dissolution textures, cementation patterns, and aragonite and Mg–calcite alteration in the Holocene Isla Cancún Eolianite aragonitic ooids: Modern analog for ancient ooid-grainstone pore networks: Gulf Coast Association of Geological Societies Journal, v. 6, p. 1–20, <https://www.gcags.org/Journal/2017.GCAGS.Journal/2017.GCAGS.Journal.v6.01.p1-20.Loucks.and.Patty.pdf>.

Lucia, F. J., 1995, Rock-fabric/petrophysical classification of carbonate pore space for reservoir characterization: American Association of Petroleum Geologists Bulletin, v. 79, p. 1275–1300.

Machel, H. G., 2004, Concepts and models of dolomitization: A critical reappraisal: Geological Society (London) Special Publications, v. 235, U.K., p. 7–63, <https://doi.org/10.1144/GSL.SP.2004.235.01.02>.

McFarlan, E., Jr., and L. S. Memes, 1991, Lower Cretaceous, *in* A. Salvador, ed., The geology of North America, v. J: The Gulf of Mexico Basin: Geological Society of America, Boulder, Colorado, p. 181–204, <https://doi.org/10.1130/DNAG-GNA-J.181>.

Melim, L. A., P. K. Swart, and R. G. Maliva, 2001, Meteoric and marine-burial diagenesis in the subsurface of Great Bahama Bank: Subsurface geology of prograding carbonate platform margin, Great Bahama Bank: Results of the Bahamas Drilling Project: Society of Economic Paleontologists and Mineralogists (Society for Sedimentary Geology), p. 131–161, <https://doi.org/10.2110/pec.01.70.0137>.

Mitchell-Tapping, H. J., 1981, Petrophysical properties of the Sligo Formation of northern Louisiana and Arkansas: Gulf Coast Association of Geological Societies Transactions, v. 31, p. 155–166.

Mitchell-Tapping, H. J., 1984, Petrology and depositional environment of the Sunniland producing fields of South Florida: Gulf Coast Association of Geological Societies Transactions, v. 34, p. 157–173.

Mitchell-Tapping, H. J., 2003, Exploration of the Sunniland Formation of southern Florida: Gulf Coast Association of Geological Societies Transactions, v. 53, p. 599–609.

Phelps, R. M., C. Kerans, R. G. Loucks, R. Da-Gama, J. Jeremiah, and D. Hull, 2013, Oceanographic and eustatic control of carbonate platform evolution and sequence stratigraphy on the Cretaceous (Valanginian-Campanian) passive margin, northern Gulf of Mexico: Sedimentology, v. 62, p. 461–496, <https://doi.org/10.1111/sed.12062>.

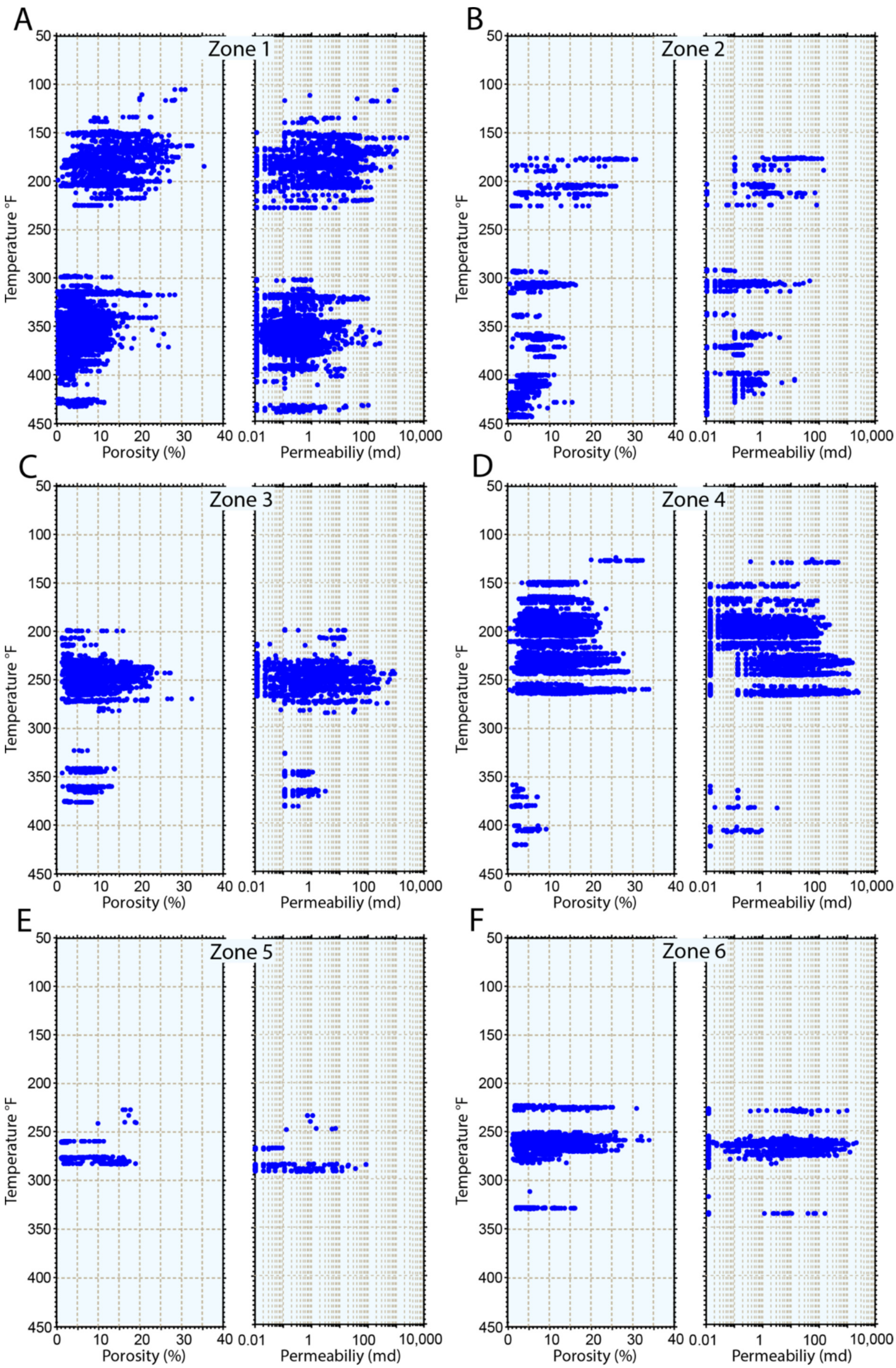
A
Zone 1
B
Zone 2
C
Zone 3
D
Zone 4
E
Zone 5
F
Zone 6
Temperature °F
50
100
150
200
250
300
350
400
450
Porosity (%)
0
10
20
30
40
Permeabiliy (md)
0.01
1
100
10,000

**(FACING PAGE) Figure 10. Porosity and permeability versus temperature by geographic zone. (A) Zone 1. (B) Zone 2. (C) Zone 3. (D) Zone 4. (E) Zone 5. (F) Zone 6.**

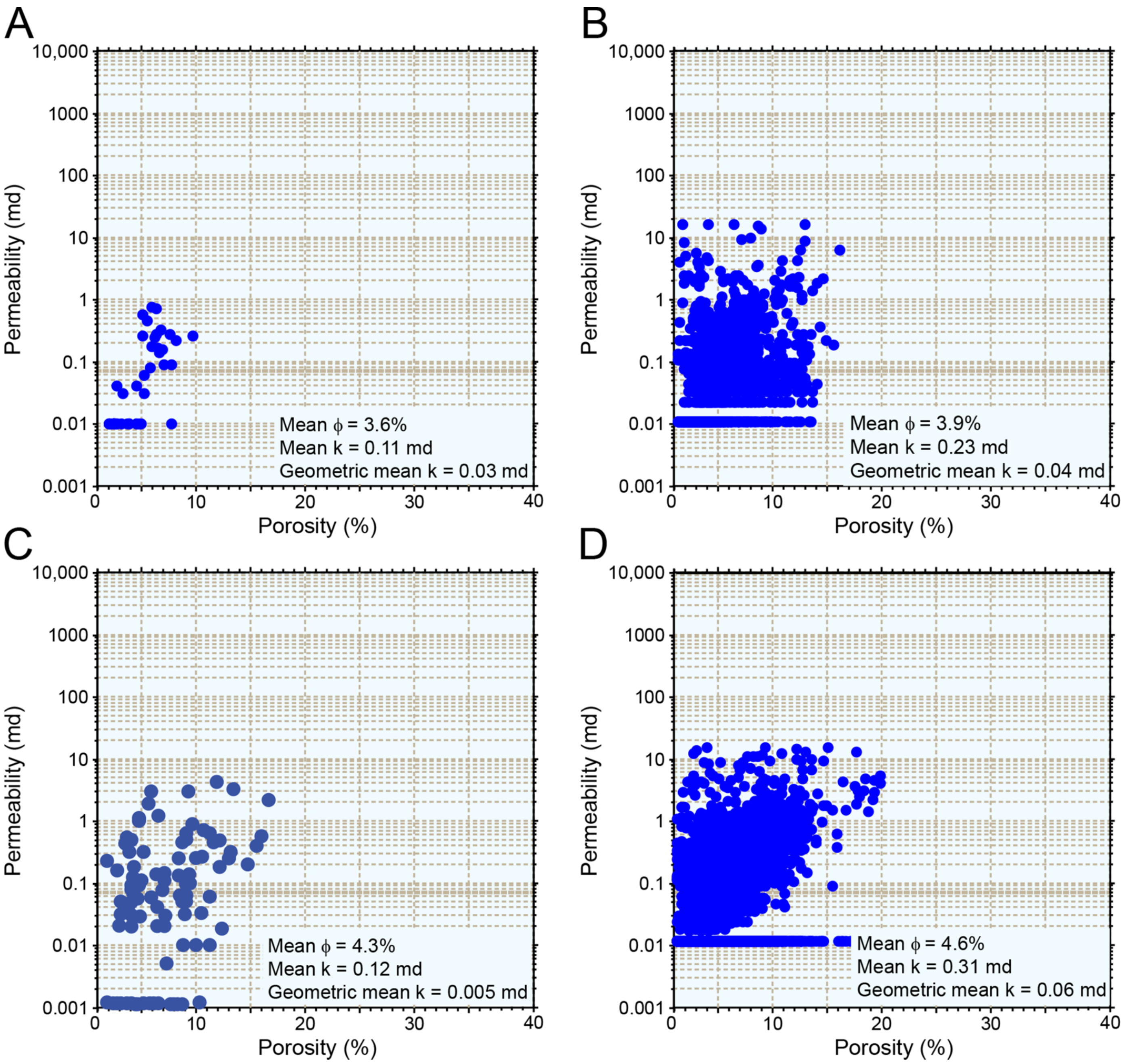


**Figure 11. Porosity versus permeability plots for case examples of micropore-dominated pore networks. (A) Calvin Limestone, Natchitoches Parish, Louisiana. (B) Sligo Reef Trend, South Texas. (C) James Limestone, Pearl County, Mississippi. (D) Stuart City Reef Trend, South Texas. Note that line at 0.01 md permeability is likely caused by inability of analytical equipment to read permeability values lower than 0.01 md.**


Schmoker, J. W., and R. B. Halley, 1982, Carbonate porosity versus depth: A predictable relation for South Florida: American Association of Petroleum Geologists Bulletin, v. 66, p. 2561–2570, <https://doi.org/10.1306/03B5AC73-16D1-11D7-8645000102C1865D>.

Scholle, P. A., and D. S. Ulmer-Scholle, 2006, A color guide to the petrography of carbonate rocks: Grains, textures, porosity, diagenesis: American Association of Petroleum Geologists Bulletin Memoir 77, Tulsa, Oklahoma, 474 p.

Soto-Kerans, P., R. G. Loucks, and C. Kerans, 2017, Lower Cretaceous Albian Platform mixed carbonate/siliciclastic strata of the Upper Glen Rose D Member in the East Texas and Brazos basins, regional setting, depositional systems, and lithofacies variability: American Association of Petroleum Geologists Search

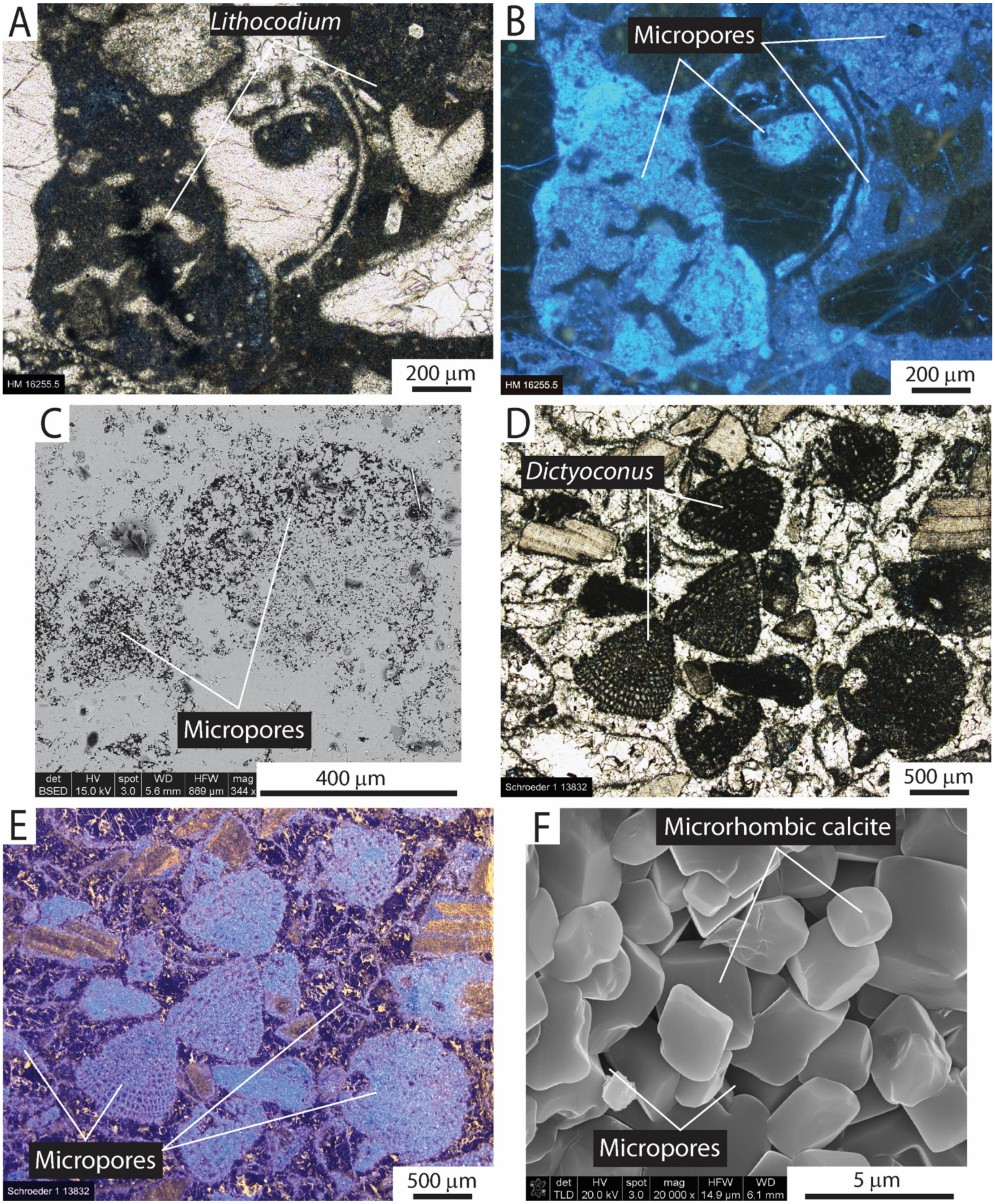
A
Lithocodium
HM 16255.5
200 μm
B
Micropores
HM 16255.5
200 μm
C
Micropores
det BSED HV 15.0 kV spot 3.0 WD 5.6 mm HFW 869 μm mag 344 x
400 μm
D
Dictyoconus
Schroeder 1 13832
500 μm
E
Micropores
Schroeder 1 13832
500 μm
F
Microrhombic calcite
Micropores
det TLD HV 20.0 kV spot 3.0 mag 20 000 x HFW 14.9 μm WD 6.1 mm
5 μm

**(FACING PAGE) Figure 12. Photomicrographs and images of micropore-dominated network case studies (from Loucks et al., 2013, reproduced with permission of the Gulf Coast Association of Geological Societies). (A) Micropores in former Mg–calcite *Lithocodium* encrusting material are the major pore type in the deeply buried Calvin Limestone. ARCO 1 Huffman McNeely (16,255.6 ft [4954.7 m]), Natchitoches Parish, Louisiana. (B) Same photomicrograph as A but under ultraviolet light, where micropores show up as blue haze. (C) SEM backscatter image of Ar–ion milled sample. Micropores appear black. Calvin Limestone, ARCO 1 Huffman McNeely (16,676 ft [5082.8 m]), Natchitoches Parish, Louisiana. (D) Micropores in the Stuart City Limestone are predominantly in former Mg–calcite grains and micrite envelopes. In this photomicrograph, the micropores are in *Dictyoconus* foraminifers and micrite envelopes. Pioneer Energy 1 Schroeder (13,832 ft [4216 m]), Bee County, Texas. (E) Same photomicrograph as D but under ultraviolet light, where micropores show up as blue haze. (F) SEM image of microrhombic calcite and associated micropores in the Stuart City Limestone. Pioneer Energy 1 Schroeder (13,029.5 ft [3971.4 m]), Bee County, Texas.**

and Discovery Article 51468, Tulsa, Oklahoma, 5 p., <http://www.searchanddiscovery.com/pdfz/documents/2018/51468soto-kerans/ndx_soto-kerans.pdf.html>.

Terriere, R. T., 1976, Geology of Fairway Field, East Texas, *in* J. Braunstein, ed., North American oil and gas fields: American Association of Petroleum Geologists Memoir 24, Tulsa, Oklahoma, p. 157–176, <https://doi.org/10.1306/M24385C12>.

Waite, L. E., 2009, Edwards (Stuart City) shelf margin of South Texas: New data, new concepts: American Association of Petroleum Geologists Search and Discovery Article 10177, Tulsa, Oklahoma, 39 p., <http://www.searchanddiscovery.com/documents/2009/10177waite/index.htm>.

Webster, R. E., D. Luttner, and L. Liu, 2008, Fairway James Lime Field, East Texas: Still developing after 48 years: American Association of Petroleum Geologists Search and Discovery Article 110061, Tulsa, Oklahoma, 40 p., <http://www.searchanddiscovery.com/pdfz/documents/2008/08092webster/ndx_webster.pdf.html>.

Zahm, L., 2010, Albian cyclic shelf tidal bar complexes, upper Glen Rose "D" formation, Alabama Ferry Field, East Texas: Gulf Coast Association of Geological Societies Transactions, v. 60, p. 771–778.

ZetaWare, 2003, ZetaWare utilities --- BHT correction, I only have time since circulation, <https://www.zetaware.com/utilities/bht/timesince.html>.

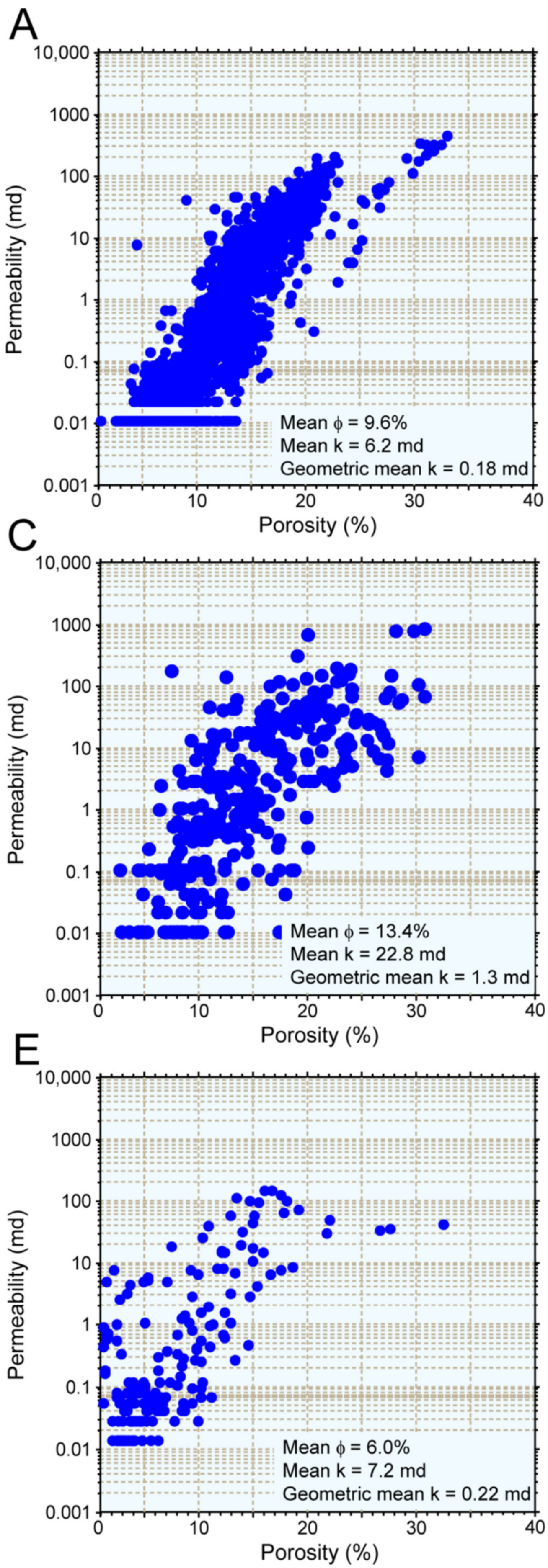


**Figure 13. Porosity versus permeability plots for case examples of macropore-dominated pore networks. (A) Pettet Limestone, Caddo Parish, Louisiana. (B) James Limestone, Fairway Field, Henderson County, Texas. (C) Sunniland Limestone, Sunniland Field, Henry and Collier counties, Florida. (D) Upper Glen Rose Limestone, Alabama Field, Leon County, Texas. (E) Cow Creek and Bexar limestones, South Texas.**

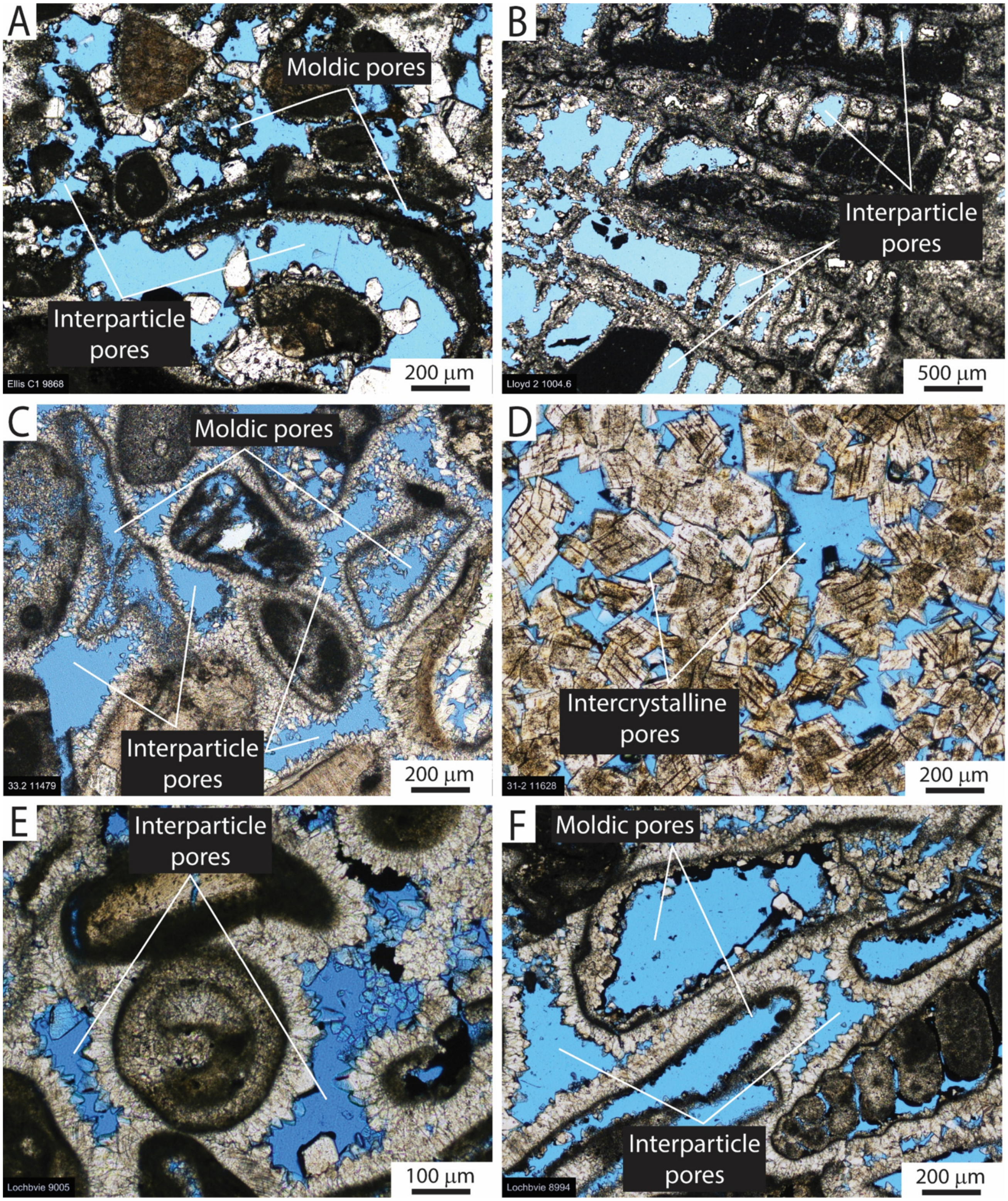


**Figure 14. Photomicrographs and images of macropore-dominated network case studies. (A) Macropores in the James Limestone are dominated by calcite-cement-reduced interparticle and moldic pores. Cities Service C–1 Ellis (9868 ft [3007.8 m]), Henderson County, Texas. (B) Corals and other allochems contain intraparticle pores. James Limestone, Sun Oil 2 Lloyd (9004.6 ft [2744.6 m]), Henderson County, Texas. (C) Sunniland grainstones, where porous, are dominated by interparticle and moldic pores. Early calcite-rim cement formed a rigid framework inhibiting compaction. Sunniland Limestone, Sun Oil 33–2 Red Cattle (11,479 ft [3498.8 m]), Henry County, Florida. (D) Some of the Sunniland strata are dolomitized to the extent that all allochems are obliterated. This type of diagenesis can develop excellent intercrystalline pores. Sunniland Limestone, Sun Oil 31–2 Red Cattle (11,628 ft [3544.2 m]), Henry County, Florida. (E) In the grainstones of the Upper Glen Rose Limestone in the Alabama Ferry Field, early, bladed, calcite-rim cement formed a rigid framework that stopped compaction, and abundant interparticle pores were preserved. Upper Glen Rose Limestone, Lasmo Energy 1 Lochbuie (9005 ft [2744.7 m]), Leon County, Texas. (F) Moldic pores formed after dissolution of former aragonite mollusk fragments are a major pore type in the Glen Rose Limestone. Upper Glen Rose Limestone, Lasmo Energy 1 Lochbuie (8994 ft [2741.1 m]), Leon County, Texas.**

**Figure 15. Plot of mean porosity versus geometric mean permeability for formations investigated in this study. The pore networks appear to separate into two types: macropore-dominated and micropore-dominated.**